Australian Government
Department of Defence
Defence Science and
Technology Organisation

Kinematic and Attribute Fusion Using a Bayesian Belief Network Framework

Mark L Krieg

Intelligence, Surveillance and Reconnaissance Division

Defence Science and Technology Organisation

DSTO–RR–0315

ABSTRACT

The focus of tracking applications has traditionally centred on kinematic state estimation. However, attribute information has the potential to not only provide identity and class information, but it may also improve data association and kinematic tracking performance. Bayesian Belief Networks provide a framework for specifying the dependencies between kinematic and attribute states. Algorithms based on this framework are developed for joint kinematic and attribute data association, kinematic tracking, attribute state estimation, and joint kinematic and attribute tracking. The algorithms are demonstrated using simulated tracking scenarios.

Published by

Defence Science and Technology Organisation
PO Box 1500
Edinburgh, South Australia 5111, Australia

Telephone: (08) 8259 5555
Facsimile: (08) 8259 6567

AR No. 013–722
August, 2006

APPROVED FOR PUBLIC RELEASE

Kinematic and Attribute Fusion Using a Bayesian Belief Network Framework

EXECUTIVE SUMMARY

The kinematic and attribute states of a target are not generally independent of each other. It is often possible to infer information about one from knowledge of the other. The use of both can improve both data association and state estimation. However, kinematic states are generally continuous and time variant, whereas attribute states are often discrete and may be static or time variant. Traditionally, the techniques used for the estimation of one may not be suitable for the other.

A Bayesian Belief Network (BBN) is a useful tool for modelling the joint probability of dependent continuous and discrete variables. As such, it can be used to specify the uncertain dependencies between the kinematic and attribute states of the target tracking and recognition problem, and it provides a framework from which data association and target state estimation algorithms may be developed. Different network topologies may be used to develop different algorithms, that is, the design of the algorithms will be influenced by the choice of network variables and the relationship between them.

The BBN framework has been applied to the development of a joint kinematic and attribute data association algorithm. The use of both kinematic and attribute sensor data and target states improves the ability of the algorithm to discriminate between multiple measurements and targets. Kinematic and attribute state estimation or tracking algorithms have also been developed using this framework. Under linear and Gaussian assumptions, it is shown that the kinematic estimator reverts to the Kalman filter. An algorithm for estimating a target's identity and class using attribute measurements is also developed. The performance of these algorithms is demonstrated using a simulated target tracking and recognition application. The improvement in the data association performance due to the availability of the attribute measurements and target attribute estimates is shown to improve the kinematic tracking performance, particularly in dense target scenarios.

A joint kinematic and attribute tracking algorithm is developed using a BBN that captures the dependencies between the target's kinematic and attribute states. Demonstration of the algorithm using simulated scenarios shows that the target's class or type can be estimated from the kinematic behaviour of the target. The knowledge of the target's class may also improve the kinematic tracking performance through the selection of the most appropriate kinematic model for that class.

Author

Mark L Krieg
Intelligence, Surveillance and Reconnaissance Division

Dr Krieg joined the Defence Science and Technology Organisation (DSTO) Australia in 1976 as an apprentice. During the 1980s, he worked as a technical officer in the areas of communication networks, and control and instrumentation. After obtaining his BE(Elect) from the University of Adelaide in 1992 and his PhD from the same institution in 1998, he joined the Microwave Radar Division in 1992, where he worked in the radar signal and data processing area. He is currently a Senior Research Scientist attached to the Tracking and Sensor Fusion group of the Intelligence, Surveillance and Reconnaissance Division, where he is pursuing research into multi-sensor tracking and fusion for defence applications.

Contents

Figures

Tables

Abbreviations and Acronyms

ATC	Air Traffic Control
BBN	Bayesian Belief Network
EKF	Extended Kalman Filter
ES	Electronic Surveillance
ESM	Electronic Support Measures
FLIR	Forward Looking Infrared
GNN	Global Nearest Neighbours
HRR	High Range Resolution
IBS	Integrated Broadcast System
ID	identification, identity
IFF	Identification Friend or Foe
IR	infrared
IRST	Infrared Search and Track
ISAR	Inverse Synthetic Aperture Radar
MAP	maximum *a posteriori*
NCTR	Non-Cooperative Target Recognition
PAS	Probabilistic Argumentation System
RCS	Radar Cross Section
RWR	Radar Warning Receiver
SATCOM	Satellite Communication
SIF	Selective Identification Feature
SSR	Secondary Surveillance Radar
TADIL	Tactical Digital Information Link

1 Introduction

The objective of any effective surveillance system is to generate a picture of the situation of interest by locating and recognising all the targets of interest within its volume of coverage. Traditional techniques treat this as two separate problems that are executed sequentially. The first problem is to estimate the position, speed and heading of the targets using the available kinematic measurements. This process is known as target tracking. The second problem is target recognition, in which the attribute measurements from the sensors and contextual information are used to determine the most likely identity (ID), class, category, and other information for the targets being tracked. The identity of a target refers to its allegiance, for example, friend, assumed friend, neutral, suspect and hostile. A target's class is the type of platform, which may be determined to varying degrees of detail, and its category is one of air, surface, ground, sub-surface or space.

The field of target tracking is well established, finding its origins in single radar tracking [Blackman & Popoli 1999]. However, automatic target recognition, which includes automatic target or track identification and automatic target classification, has attracted increased interest since the advent of multiple sensor tracking and data fusion. The fusion of data from multiple sensors provides disparate attribute information that may be useful for discriminating between different classes and identities. For example, a Secondary Surveillance Radar (SSR) provides identification codes from transponder interrogations and an Electronic Surveillance (ES) sensor contributes to platform classification through the detection and identification of emitters.

The separation of kinematic tracking and attribute state estimation assumes that the two are independent. Although this assumption simplifies the problem, potentially significant information from one of target tracking or target recognition is not available for the other. In particular, the location, altitude and speed of a target, and the target's ability to manoeuvre, may provide insight into the target's category, identity or class. For example, a Hornet F/A–18 may reach speeds in excess of Mach 1 and perform manoeuvres with acceleration greater than $5\,g$, whereas a Boeing 747 will not. Similarly, knowledge of a platform's class may allow a tracker to select more appropriate dynamic models to improve its kinematic tracking performance. The use of both kinematic and attribute information for associating sensor measurements or plots to tracks may provide greater discrimination between data and reduce the incidence of incorrect association.

A target's kinematic state space and kinematic measurements are generally continuous valued entities, whereas the target's attributes and the sensor attribute measurements may be either continuous or discrete. For example, Radar Cross Section (RCS) and target size may be continuous, but the platform type and category are discrete. Furthermore, both the measurements and target state estimates are uncertain. A Bayesian Belief Network (BBN) has the capability to accommodate both continuous variables to represent a target's kinematic information and discrete variables to represent its identity and class information, making it a suitable candidate for target tracking and recognition applications. The underlying Bayesian probability calculus provides the mechanism for handling state uncertainty and errors. Thus, BBNs provide a rigorous basis, or framework, for developing (joint) tracking and recognition algorithms.

This report addresses the development of kinematic and attribute data association and state estimation algorithms, using the BBN as the basis for defining the state and measurement variables and the dependencies between them. The BBN is not directly implemented as the solution, rather it may be thought of as a tool used for the development of the algorithms, with the network topology defining the posterior probability of the output state variables. This, and the method used to determine the most probable values for the output state variables, dictate the design of the resulting algorithm. This approach is used to develop data association algorithms using both kinematic and attribute measurements and state variables, a kinematic state estimation algorithm using kinematic measurements, and an attribute state estimation algorithm using attribute measurements. The latter is demonstrated using a target identification and classification application. Finally, a joint target tracking and classification algorithm, in which both the kinematic and attribute measurements are used to jointly estimate the target dynamics and class, is developed. Although the algorithms are developed for target tracking and recognition applications, the BBN formulation allows the dependencies between any state and measurement variables to be defined, and provides a mechanism for developing similar algorithms for other scenarios and applications.

Following this introduction, the relevant background material is presented in Section 2, and a brief description of BBNs follows in Section 3. The data association algorithms are developed and evaluated in Section 4. Similarly, the state estimation algorithms and the joint tracking and recognition algorithms are presented in Sections 5 and 6, respectively. Finally, the conclusions are presented in Section 7.

2 Background

In general, a typical sensor will provide at least partial kinematic information. It may also provide attribute data that supports the estimation of non-kinematic states, such as identity, class, and category. For example, primary radars may provide range, bearing, elevation and Doppler velocity measurements and may also provide classification information through Non-Cooperative Target Recognition (NCTR) techniques that use the propeller or jet engine modulation of the Doppler frequency. Specialist radar modes, such as High Range Resolution (HRR) and Inverse Synthetic Aperture Radar (ISAR) provide additional classification capabilities. Secondary radars are used extensively for Air Traffic Control (ATC) in the civilian domain and Identification Friend or Foe (IFF) for target identification in military applications. These sensors provide bearing and range measurements, and identification and altitude information through Selective Identification Feature (SIF) codes. Electronic Surveillance (ES) sensors, such as Electronic Support Measures (ESM) and Radar Warning Receivers (RWRs) may provide bearing and elevation measurements, and emitter and platform classification information. An infrared (IR) sensor, such as a Forward Looking Infrared (FLIR) or a Infrared Search and Track (IRST), provides accurate bearing, elevation and, if fitted with a laser range finder, range measurements. The availability of target size information may contribute to target recognition. Tactical Digital Information Link (TADIL), Satellite Communication (SATCOM) protocols, such as the Integrated Broadcast System (IBS), and other data communication links are potential sources of attribute information. In addition, prior or contextual information, such as the

location of air-bases, flight paths and air corridors, may also contribute to the estimation of attribute states.

Although both kinematic and attribute target state information provide useful information for compiling the situational picture, a number of significant differences exist between the two. A target's kinematic state, which is primarily its position and velocity, is generally continuous and time variant. On the other hand, the attribute states may be either continuous or discrete, and either time varying or time invariant. For example, RCS is continuous and time variant, whereas identity is discrete and time invariant. The target attributes may be categorised as either *evolutionary* or *non-evolutionary*, for time varying or time invariant, respectively [Blackman & Popoli 1999]. The sensor measurements may be similarly categorised.

The two key challenges are to successfully combine the disparate data or information, and to handle the errors or uncertainty in the data. Bayesian techniques and Dempster-Shafer theory are two prevailing approaches that are able to accommodate these challenges. Bayesian techniques use Bayesian probability theory to handle the uncertainty, whereas Dempster-Shafer introduces the concepts of support and plausibility [Bogler 1987, Simard, Couture & Bossé 1996]. Bayesian probability theory provides a common frame of reference for the kinematic and attribute variables, and has previously been exploited for joint tracking and classification [Challa & Pulford 1999, Gordon, Maskell & Kirubarajan 2002, Krieg 2003*a*].

Bayesian techniques involve determining the posterior probability of the variables of interest, and then applying estimation techniques, such as maximum *a posteriori* (MAP), to determine the most likely state from the posterior distribution. The difficulty is defining the posterior probability, which may involve the joint probability of all the variables in the system. Bayesian Belief Networks (BBNs) are causal belief networks that model the dependencies between the variables, represented by network nodes, using Bayesian probability [Pearl 1988], and only require the user to know the dependence relationships between directly connected nodes or variables. In addition, the ability to accommodate continuous variables to represent kinematic information and discrete variables to represent identity and class information make them a suitable candidate for multiple source target tracking and recognition applications [Stewart & McCarty 1992]. However, the dependencies between attributes generally produce non-singly connected networks for attributes that evolve over time [Hautaniemi, Korpisaari & Saarinen 2000], which generally require the use of techniques such as clustering, conditioning or stochastic simulation to guarantee convergence to the global solution [Pearl 1988].

BBNs have been applied to a number of multiple source tracking related applications. For example, Korpisaari & Saarinen [1999] proposed a generalised Bayesian network structure with a many-dimensional association vector for applying attribute data in a Joint Probabilistic Data Association (JPDA) context, and Chang & Fung [1997] used a BBN to incorporate attribute information into a multiple hypothesis tracking algorithm in which attributes are used to solve both the association and track update problems. Krieg showed how BBNs may be used as a basis for deriving the Kalman filter tracking algorithm, and used BBNs to develop an attribute estimation algorithm [Krieg 2002], various joint kinematic and attribute data association algorithms [Krieg 2003*b*], and a joint kinematic and attribute tracking solution [Krieg 2003*a*].

3 Bayesian Belief Networks

A Bayesian belief network (BBN) is a causal network comprising a set of nodes connected by directed links or arcs. The nodes of the network represent the stochastic variables of a system or domain, and the directed arcs between the nodes represent the direct causal influences between the variables [Jensen 1996]. Connected nodes are deemed to have a *cause* and *effect*, or *parent* and *child*, relationship, with the direction of the arc being from cause to effect, or parent node to child node. Any node without at least one parent node is known as a root node, and any node with no child nodes is referred to as a leaf node.

The BBN provides a complete probabilistic model of all the variables in the domain of interest. Although it may be difficult to conceptualise the overall interaction between all the variables, the construction of the BBN is based on the local interactions between the variables that directly influence one another. Therefore it is only necessary to determine the conditional probabilities for each variable, that is, the probability given the state of each of its direct causes or parent nodes [Pearl 1988]. This is conceptually simpler than attempting to define the joint probability of all the variables in the domain.

The independence between the variables of a BBN is introduced through the concept of *d-separation* [Jensen 1996]. Within a BBN, some knowledge of the state of a variable may be inferred from the state of another variable. However, if the states of all the variables in all the paths separating the two variables are known, then the knowledge of the state of one will not provide any additional insight into the state of the other, and the two variables become independent. Similarly, if the state of a particular node is known, then its child nodes are independent. The situation differs for the variables sharing a common child node; the parent nodes are only independent if there is no knowledge of the state of the child or any of its descendants. Another distinction is that only partial, or soft, knowledge is necessary for dependence in this case, as opposed to the two former, where complete, or hard, knowledge is required for independence.

The objective is to determine the posterior probability, or *belief*, of the state of variables of interest in the network, subject to the application of the available knowledge of the state of a subset of the nodes of the network; herein referred to as evidence. This posterior probability is dynamically calculated from the static prior and conditional probabilities, and any evidence that has been applied to, and propagated through, the network. By definition, the evidence is propagated in the direction of the causal links using π messages and against the direction of the links using λ messages. On receipt of a message from one of the nodes directly connected to it, a node will update its belief and propagate new messages to each of the other nodes directly connected to it, thereby ensuring the evidence is propagated throughout the network. The belief at any node is the normalised product of the λ and π information at that node.

In this report it is assumed, without loss of generality, that evidence is only applied to the network as leaf nodes. To avoid convergence and deadlock issues related to loops in the underlying Markov network, propagation is only considered for tree structured networks, that is, those for which each variable has only one parent node. Non-complying networks are converted to tree structures by clustering or aggregating nodes [Pearl 1988, Krieg 2001]. Unless stated otherwise, a node or variable is denoted by an uppercase alphabetic character, and its value is denoted by its lowercase equivalent.

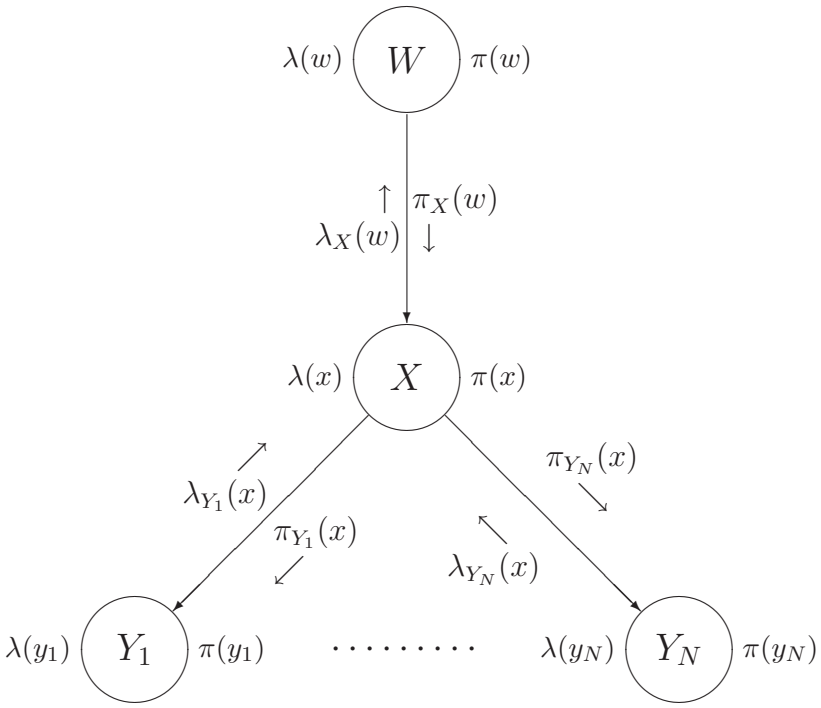

Figure 1: *Evidence propagation in a BBN*

3.1 Propagation in Bayesian Belief Networks

To illustrate the propagation of evidence in a BBN, consider the network of Figure 1. The total evidence or information, e_X, influencing the proposition that the node X has the value x, that is, $X = x$, is separated into two disjoint subsets, e_X^+ denoting the evidence introduced through the arc between the node X and its parent node, W, and e_X^-, denoting the evidence introduced to the node X through the arcs between it and its children, $Y_1, \ldots, Y_N$. The specific evidence introduced through the arc to child Y_i, $i = 1, 2, \ldots, N$, is denoted $e_{XY_i}^-$.

For the root node, W, the evidence e_W^+ is the background knowledge or prior probability of all the possible values for that node, $\mathtt{p}(W = w), \forall w$, which is denoted $\mathtt{p}(w)$ for notational expediency. In the case of the leaf nodes, Y_i, $i = 1, \ldots, N$, $e_{Y_i}^-$ may take one of three forms, namely:

1. no evidence, where the possible values of the node Y_i are uniformly distributed, that is, $\mathtt{p}(y_i) = \frac{1}{N_{y_i}}$, where N_{y_i} is the number of possible values of Y_i for discrete variables or the difference between the maximum and minimum values for continuous variables;

2. soft evidence, where the probability of each possible value of Y_i is provided, generally as a probability mass function for discrete variables or a probability density function for continuous variables; or

3. hard evidence, where the value of the node Y_i is known, that is, $\mathtt{p}(y_i) = \delta_{y_i y_i'}$, where y_i' is the known value of Y_i and $\delta_{y_i y_i'}$ is the Kronecker Delta function, which equals 1 when $y_i = y_i'$ and zero otherwise.

Assuming that e_X^- and e_X^+ are independent, which is supported by the concept of *d-separation* [Jensen 1996], and applying Bayes' Rule, the belief that $X = x$ is

$$\mathrm{Bel}(x) = \mathtt{p}\left(x|e_X^-, e_X^+\right) = \frac{\mathtt{p}\left(e_X^-|x\right)\mathtt{p}\left(x|e_X^+\right)}{\sum_x \mathtt{p}\left(e_X^-|x\right)\mathtt{p}\left(x|e_X^+\right)},$$

where $\sum_x$ is the summation over all the possible values of the node X. Defining $\pi(x) = \mathtt{p}\left(x|e_X^+\right)$ and $\lambda(x) = \mathtt{p}\left(e_X^-|x\right)$, this becomes

$$\mathrm{Bel}(x) = \alpha\,\pi(x)\lambda(x), \tag{1}$$

where $\lambda(x)$ is the likelihood representing the *diagnostic* or *retrospective* support for the proposition $X = x$, $\pi(x)$ is the prior probability representing the *causal* or *predictive* support for $X = x$, and α is a normalising constant.

Consider the propagation of the λ messages in Figure 1. The retrospective support provided by the evidence on each leaf node Y_i, $i = 1, \ldots, N$ is contained in the message $\lambda_{Y_i}(x)$, which is defined as

$$\lambda_{Y_i}(x) = \sum_{y_i} \mathtt{p}\left(y_i|x\right)\lambda(y_i), \tag{2}$$

where $\mathtt{p}\left(y_i|x\right)$ is the probability that $Y_i = y_i$ conditioned on $X = x$. The total retrospective support for the proposition $X = x$ is obtained by aggregating the retrospective support from all the child nodes of X using

$$\lambda(x) = \prod_{i=1}^{N} \lambda_{Y_i}(x). \tag{3}$$

The retrospective support is then propagated to the parent of X according to

$$\lambda(w) = \sum_x \mathtt{p}\left(x|w\right)\lambda(x). \tag{4}$$

The predictive support is propagated by the π messages in the direction of the links. The support provided by the root node W is simply the prior probability of W, that is, $\pi(w) = \mathtt{p}\left(w\right)$. This is propagated to the node X using

$$\pi(x) = \sum_w \mathtt{p}\left(x|w\right)\pi(w). \tag{5}$$

From X, the predictive support is propagated to the child nodes of X, namely Y_i, $i = 1, \ldots, N$, as

$$\pi_{Y_i}(x) = \prod_{k=1\setminus i}^{N} \lambda_{Y_k}(x)\pi(x) = \frac{\mathrm{Bel}(x)}{\lambda_{Y_i}(x)}, \tag{6}$$

where $\setminus$ denotes the *setminus* operator, that is, $\prod_{k=1\setminus i}^{N}$ is the product over the values $k = 1, \ldots, i-1, i+1, \ldots, N$.

Having now propagated both the predictive and retrospective support throughout the BBN, the posterior probability of each possible value for each node may be calculated as the normalised product of the predictive and retrospective support of that node. The process is repeated whenever further evidence is applied to the network.

4 Data Association

Traditional data association using kinematic data provides limited discrimination in the measurement space, which is usually of a lower dimension than the track state space. Although sufficient for sparse target scenarios, dense target scenarios may produce ambiguous solutions that have the potential to lead to poor association performance. The use of attribute data has the potential to increase the discrimination in the measurement space. For example, an ESM system may provide bearing measurements and emitter identification information. The bearing alone often provides inadequate discrimination, and the additional discrimination provided by the emitter identification has the potential to resolve some, if not all, the ambiguities. However, a consistent distance measure must be applied to all elements used in the association. The traditional squared distance metric used for kinematic data does not readily apply to attribute data. These distance metrics are a simplification of a probability based on Gaussian distributions, where the squared distance appears in the exponent. In the case where all stochastic variables are Gaussian distributed, the smallest distance corresponds to the maximum probability.

This section considers two approaches to data association, namely unconstrained and constrained. The former treats all measurements at a particular time, or within a single scan, independently. As such, the association is unconstrained, and is referred to here as *unconstrained measurement-to-track association*. The latter treats all the measurements at a particular time, or from a single scan, as a block of measurements. This relaxation of the assumption of independence between the measurements allows the introduction of constraints on the association solution, such as permitting only one measurement from each sensor at a particular time or scan to be associated with any one track. This is referred to here as *constrained measurement-to-track association*.

4.1 Unconstrained Measurement-to-Track Association

In unconstrained data association, each measurement is treated in isolation, and the problem becomes one of associating a single measurement with any one of M tracks at time t. This is modelled by the BBN of Figure 2, where the measurement is represented by the node Z_t, and the states of the M tracks are represented by each of the nodes $X_t^{(1)}, \ldots, X_t^{(M)}$. The association node K_t represents a discrete variable whose value is the number of the track to which the measurement is associated, that is, a track index for that measurement. The association problem is now simply one of estimating the state of K_t. This involves determining the posterior probabilities for each possible state of K_t and using the maximum *a posteriori* approach of selecting the state with the greatest probability. This is expressed mathematically as $\arg\max_{k_t} \mathsf{p}\left(k_t | z_t, x_t^{(1)}, \ldots, x_t^{(M)}\right)$. Although the formulation in Figure 2 shows a single measurement at time t, this does not restrict the

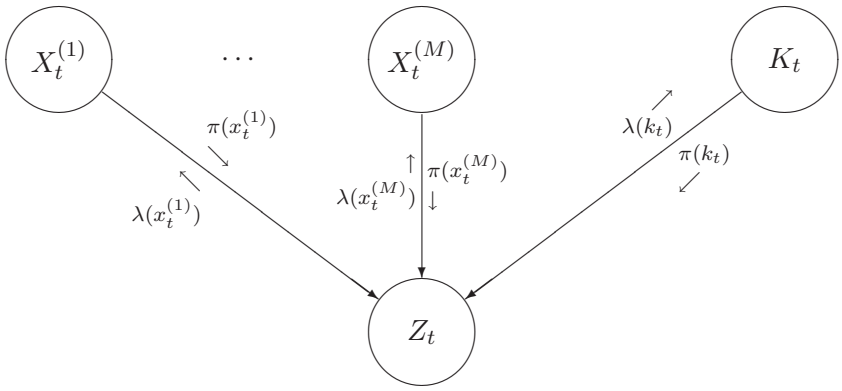

Figure 2: *BBN representation of the data association problem*

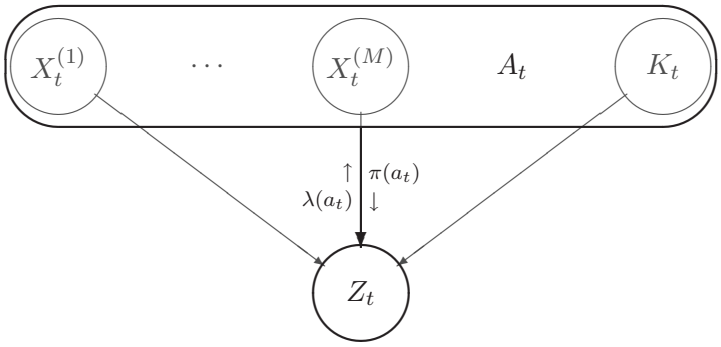

Figure 3: *Clustered BBN representation of the data association problem*

problem to a single measurement at any specific time; simultaneous measurements may be processed sequentially.

The BBN of Figure 2 is not a tree structure by virtue of the multiple parents of the node Z_t. Clustering [Pearl 1988, Krieg 2001] is used to obtain the structure of Figure 3, in which the probability of the new composite variable A_t represents the joint probability of the variables $X_t^{(1)}, \ldots, X_t^{(M)}$ and K_t.

Assuming that the prior probabilities of the track states and K_t are independent, which is reasonable if no measurement is associated with more than one track, the posterior probability that A_t will be in a particular state is the belief of that state, namely

$$\mathtt{p}\left(a_t|z_t\right) \equiv \mathrm{Bel}(a_t) = \alpha\lambda(a_t)\pi(a_t), \tag{7}$$

where $\pi(a_t)$ is the prior probability

$$\mathtt{p}\left(a_t\right) = \mathtt{p}\left(x_t^{(1)}, \ldots, x_t^{(M)}, k_t\right) = \mathtt{p}\left(k_t\right) \prod_{m=1}^{M} \mathtt{p}\left(x_t^{(m)}\right). \tag{8}$$

The track states are simply the state of the most recent update extrapolated to the time t, that is, to the time of the current measurement. The extrapolated or predicted track state probabilities may be more accurately denoted $\mathtt{p}\left(x_t^{(m)}|Z^{t-1}\right)$, where the posterior probability's dependence on the set of measurements up to the time $t-1$, that is, Z^{t-1}, is explicit (or, more accurately, the subset of measurements from Z^{t-1} that are associated with the m^{th} track).

Assume that $\lambda(z_t) = \delta_{z_t z_t'}$ and that the measurement is produced from one or more targets represented by a single track. Then

$$\mathtt{p}\left(z_t|a_t\right) = \mathtt{p}\left(z_t|x_t^{(1)},\ldots,x_t^{(M)},k_t\right) \equiv \mathtt{p}\left(z_t|x_t^{(k_t)}\right) \tag{9}$$

and, using (4), the retrospective support becomes

$$\lambda(a_t) = \sum_z \mathtt{p}\left(z_t|a_t\right)\lambda(z_t) = \mathtt{p}\left(z_t'|x_t^{(k_t)}\right). \tag{10}$$

Substituting (8) and (10) into (7), the belief that $A_t = a_t$ may be written

$$\mathrm{Bel}(a_t) = \alpha\mathtt{p}\left(z_t'|x_t^{(k_t)}\right)\mathtt{p}\left(k_t\right)\prod_{m=1}^{M}\mathtt{p}\left(x_t^{(m)}|Z^{t-1}\right). \tag{11}$$

The belief of the node K_t may now be obtained by integrating the target states out of the composite variable A_t, that is,

$$\begin{aligned}\mathrm{Bel}(k_t) &= \alpha\mathtt{p}\left(k_t\right)\int_{x_t^{(k_t)}}\mathtt{p}\left(z_t'|x_t^{(k_t)}\right)\mathtt{p}\left(x_t^{(k_t)}|Z^{t-1}\right)dx_t^{(k_t)} \\ &\quad\times\prod_{m=1\backslash k_t}^{M}\int_{x_t^{(m)}}\mathtt{p}\left(x_t^{(m)}|Z^{t-1}\right)dx_t^{(m)}, \\ &= \alpha\mathtt{p}\left(k_t\right)\int_{x_t^{(k_t)}}\mathtt{p}\left(z_t'|x_t^{(k_t)}\right)\mathtt{p}\left(x_t^{(k_t)}|Z^{t-1}\right)dx_t^{(k_t)},\end{aligned} \tag{12}$$

where

$$\alpha = \left(\sum_{k_t}\mathtt{p}\left(k_t\right)\int_{x_t^{(k_t)}}\mathtt{p}\left(z_t'|x_t^{(k_t)}\right)\mathtt{p}\left(x_t^{(k_t)}|Z^{t-1}\right)dx_t^{(k_t)}\right)^{-1}. \tag{13}$$

Assuming uniform prior probabilities for K_t, (13) may be written

$$\mathrm{Bel}(k_t) = \frac{\int_{x_t^{(k_t)}}\mathtt{p}\left(z_t'|x_t^{(k_t)}\right)\mathtt{p}\left(x_t^{(k_t)}|Z^{t-1}\right)dx_t^{(k_t)}}{\sum_{m=1}^{M}\int_{x_t^{(m)}}\mathtt{p}\left(z_t'|x_t^{(m)}\right)\mathtt{p}\left(x_t^{(m)}|Z^{t-1}\right)dx_t^{(m)}}. \tag{14}$$

This result is consistent with the concept of d-separation, where the knowledge of the node Z_t allows knowledge of the state of the node K_t to be inferred from the knowledge of the track states.

For the special case of continuous linear Gaussian systems, (14) becomes

$$\mathrm{Bel}(k_t) = \frac{\det\left(D(k_t)\right)^{-\frac{1}{2}} \exp\left(-\frac{1}{2}\left(z'_t - Hx_t^{(k_t)}\right)^{\mathrm{T}} D(k_t)^{-1}\left(z'_t - Hx_t^{(k_t)}\right)\right)}{\sum_{m=1}^{M} \det\left(D(m)\right)^{-\frac{1}{2}} \exp\left(-\frac{1}{2}\left(z'_t - Hx_t^{(m)}\right)^{\mathrm{T}} D(m)^{-1}\left(z'_t - Hx_t^{(m)}\right)\right)}, \quad (15)$$

where $D(i) = HP_t^{(i)}H^{\mathrm{T}} + R$, $P_t^{(i)}$ is the error covariance of the track state estimate $x_t^{(i)}$, H is the measurement matrix that maps the measurement space onto the track state space, and R is the error covariance of the measurement z_t. This result is similar to the *nearest neighbours* approach for kinematic association, as maximising the probability is equivalent minimising the argument of the exponential.

If the state and measurements can be separated into independent kinematic and attribute components, for example, states $x_t^{(k_t)}$ and $w_t^{(k_t)}$ with measurements z_t and y_t, respectively, (14) may be written as the normalised product of the kinematic and attribute posterior probabilities. Assuming continuous kinematic states and discrete attribute states, this gives

$$\mathrm{Bel}(k_t) = \gamma_t \int_{x_t^{(k_t)}} \mathtt{p}\left(z'_t|x_t^{(k_t)}\right) \mathtt{p}\left(x_t^{(k_t)}|Z^{t-1}\right) dx_t^{(k_t)} \sum_{w_t^{(k_t)}} \mathtt{p}\left(y'_t|w_t^{(k_t)}\right) \mathtt{p}\left(w_t^{(k_t)}|Y^{t-1}\right), \quad (16)$$

where

$$\gamma_t = \left(\sum_{m=1}^{M} \int_{x_t^{(m)}} \mathtt{p}\left(z'_t|x_t^{(m)}\right) \mathtt{p}\left(x_t^{(m)}|Z^{t-1}\right) dx_t^{(m)} \sum_{w_t^{(m)}} \mathtt{p}\left(y'_t|w_t^{(m)}\right) \mathtt{p}\left(w_t^{(m)}|Y^{t-1}\right)\right)^{-1}.$$

This allows the attribute and kinematic information to be treated separately before combining into a single probabilistic metric.

4.2 Constrained Measurement-to-Track Association

The single measurement problem is now expanded to one of associating N measurements at some time t to M tracks. This is represented by the BBN of Figure 4, where the N measurements are denoted as $z_t^{(n)}$, $n = 1, 2, \ldots, N$, and the track states as $x_t^{(m)}$, $m = 1, 2, \ldots, M$. The association variable, K_t, is now the $N \times 1$ vector, $k_t = (k_t^{(1)}, k_t^{(2)}, \ldots, k_t^{(N)})^{\mathrm{T}}$, $k_t^{(n)} \in \{0, 1, 2, \ldots, M\}$, where the value of the n^{th} element is the number of the track to which the n^{th} measurement is associated. A value of 0 indicates that the measurement is not associated to any track. This may occur if one or more of the following conditions apply.

1. The number of measurements exceeds the number of tracks ($N > M$) and the constraint that each target may only produce one measurement is enforced.

2. A false alarm may occur with probability greater than zero.

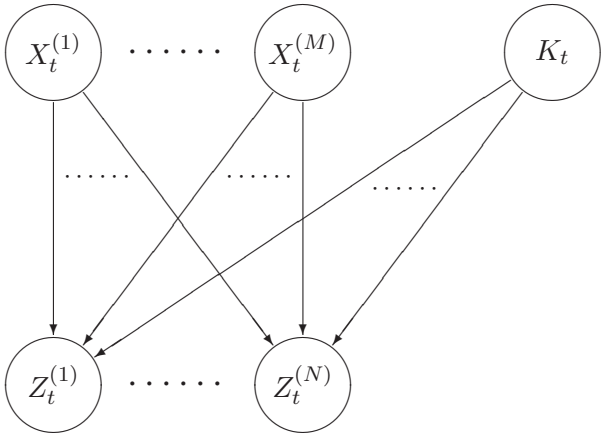

Figure 4: *BBN for associating measurements to tracks*

3. A track initiation event may occur with probability greater than zero.

As in the former case, the solution is obtained by estimating the value of k_t.

The BBN of Figure 4 contains loops in the underlying Markov network that have the potential to introduce deadlock conditions that prevent convergence to the optimal solution. The clustering technique [Pearl 1988] is again used to overcome this problem, producing the tree structured BBN of Figure 5. As for the unconstrained case, the clustered variable comprises the target states and the association variable, that is, $A_t = \{X_t^{(1)}, X_t^{(2)}, \ldots, X_t^{(M)}, K_t\}$. The predictive support for $A_t = a_t$ is simply its prior probability, namely

$$\pi(a_t) = \mathtt{p}\,(a_t) = \mathtt{p}\,(k_t) \prod_{m=1}^{M} \mathtt{p}\left(x_t^{(m)} | Z^{t-1}\right). \tag{17}$$

As before, it is assumed that the prior probabilities of the track states and the association variable are independent, which is valid under the assumption that a measurement can only be associated with a single track. This should be reflected in the prior probability of k_t, which should be zero for any values containing multiple instances of the same track number, with the exception of the value 0, for which multiple occurrences are allowed.

To obtain the solution, denote the known value of $z_t^{(n)}$ as $z_t^{(n)\prime}$, the retrospective support as

$$\lambda(z_t^{(n)}) = \delta_{z_t^{(n)} z_t^{(n)\prime}}, \tag{18}$$

and the conditional probabilities as

$$\mathtt{p}\left(z_t^{(n)} | a_t\right) = \mathtt{p}\left(z_t^{(n)} | x_t^{\left(k_t^{(n)}\right)}\right), \qquad n = 1, 2, \ldots, N. \tag{19}$$

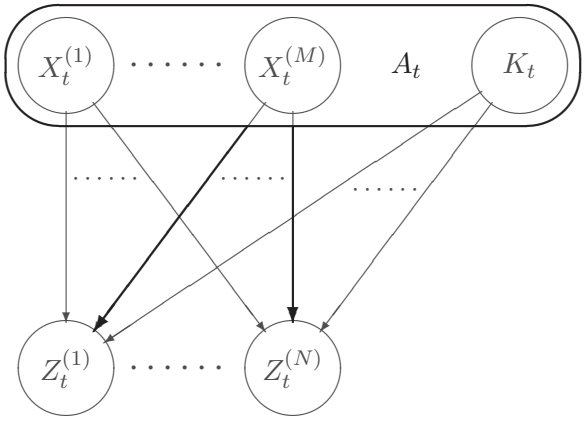

Figure 5: *Clustered BBN for associating N measurements to M tracks*

Substituting this and (18) into (2), the retrospective support for $A_t = a_t$ from the n^{th} measurement becomes

$$\lambda_{Z_t^{(n)}}(a_t) = \mathtt{p}\left(z_t^{(n)\prime}|x_t^{\left(k_t^{(n)}\right)}\right), \tag{20}$$

where $\mathtt{p}\left(z_t^{(n)\prime}|x_t^{(0)}\right)$ may be viewed as the probability of false alarm or new track. From (3), the support for $A_t = a_t$ from all measurements is

$$\lambda(a_t) = \prod_{n=1}^{N} \mathtt{p}\left(z_t^{(n)\prime}|x_t^{\left(k_t^{(n)}\right)}\right). \tag{21}$$

Invoking (1) with (17) and (21) gives the belief of $A_t = a_t$ as

$$\text{Bel}(a_t) = \alpha \mathtt{p}(k_t) \prod_{m=1}^{M} \mathtt{p}\left(x_t^{(m)}|Z^{t-1}\right) \prod_{n=1}^{N} \mathtt{p}\left(z_t^{(n)\prime}|x_t^{\left(k_t^{(n)}\right)}\right). \tag{22}$$

The belief of $K_t = k_t$ may now be found by marginalising A_t, that is,

$$\begin{aligned}
\text{Bel}(k_t) &= \alpha \mathtt{p}(k_t) \int_{x_t^{(1)}} \cdots \int_{x_t^{(M)}} \prod_{m=1}^{M} \mathtt{p}\left(x_t^{(m)}|Z^{t-1}\right) \prod_{n=1}^{N} \mathtt{p}\left(z_t^{(n)\prime}|x_t^{\left(k_t^{(n)}\right)}\right) dx_t^{(M)} \ldots dx_t^{(1)} \\
&= \alpha \mathtt{p}(k_t) \prod_{\substack{m \in k_t \\ m \neq 0}} \int_{x_t^{(m)}} \mathtt{p}\left(x_t^{(m)}|Z^{t-1}\right) \prod_{n:k_t^{(n)}=m} \mathtt{p}\left(z_t^{(n)\prime}|x_t^{(m)}\right) dx_t^{(m)} \\
&\quad \times \prod_{\substack{m' \notin k_t \\ 1 \leq m' \leq M}} \int_{x_t^{(m')}} \mathtt{p}\left(x_t^{(m')}|Z^{t-1}\right) dx_t^{(m')} \prod_{n':k_t^{(n')}=0} \mathtt{p}\left(z_t^{(n')}|x_t^{(0)}\right).
\end{aligned} \tag{23}$$

Given the constraint that each target can only produce one measurement, this reduces to

$$\begin{aligned}\mathrm{Bel}(k_t) = \alpha \mathtt{p}\left(k_t\right) \prod_{\substack{n=1 \\ k_t^{(n)} \neq 0}}^{N} \int\limits_{x_t^{\left(k_t^{(n)}\right)}} \mathtt{p}\left(z_t^{(n)\prime} | x_t^{\left(k_t^{(n)}\right)}\right) \mathtt{p}\left(x_t^{\left(k_t^{(n)}\right)} | Z^{t-1}\right) dx_t^{\left(k_t^{(n)}\right)} \\ \times \prod_{n' : k_t^{(n')} = 0} \mathtt{p}\left(z_t^{(n')} | x_t^{(0)}\right),\end{aligned} \tag{24}$$

where α is a normalising constant given by

$$\begin{aligned}\alpha^{-1} = \sum_{k_t} \mathtt{p}\left(k_t\right) \prod_{\substack{n=1 \\ k_t^{(n)} \neq 0}}^{N} \int\limits_{x_t^{\left(k_t^{(n)}\right)}} \mathtt{p}\left(z_t^{(n)\prime} | x_t^{\left(k_t^{(n)}\right)}\right) \mathtt{p}\left(x_t^{\left(k_t^{(n)}\right)} | Z^{t-1}\right) dx_t^{\left(k_t^{(n)}\right)} \\ \times \prod_{n' : k_t^{(n')} = 0} \mathtt{p}\left(z_t^{(n')} | x_t^{(0)}\right).\end{aligned} \tag{25}$$

Using the most probable value as the best estimate for the association vector, α may be ignored, and the solution is simply

$$\begin{aligned}\hat{k}_t = \arg\max_{k_t} \ \mathtt{p}\left(k_t\right) \prod_{\substack{n=1 \\ k_t^{(n)} \neq 0}}^{N} \int\limits_{x_t^{\left(k_t^{(n)}\right)}} \mathtt{p}\left(z_t^{(n)\prime} | x_t^{\left(k_t^{(n)}\right)}\right) \mathtt{p}\left(x_t^{\left(k_t^{(n)}\right)} | Z^{t-1}\right) dx_t^{\left(k_t^{(n)}\right)} \\ \times \prod_{n' : k_t^{(n')} = 0} \mathtt{p}\left(z_t^{(n')} | x_t^{(0)}\right).\end{aligned} \tag{26}$$

Again, this may be split into kinematic and attribute components.

The key assumption of a maximum of one measurement associated to each track underpins this treatment. Therefore, the prior probability mass function of the association vector must define zero probability for all values that violate this assumption. Under linear and Gaussian assumptions, the solution is effectively a Global Nearest Neighbours (GNN) association algorithm for kinematic and attribute data.

4.3 Simulation Results

The utility of joint kinematic and attribute association is demonstrated in the following simulated scenario. The scenario comprises two crossing straight line target trajectories. Range, azimuth and identity measurements are provided by a Secondary Surveillance Radar (SSR), and an Electronic Surveillance (ES) sensor provides azimuth and platform class or type measurements. Although the primary focus of the analysis of this section is the performance of the data association algorithms, state estimates are required by the data association algorithms at each time step. For convenience, the kinematic tracking is performed using an Extended Kalman Filter (EKF), which provides a linear approximation to the non-linear measurement function, and the identity and class of the targets is updated

Table 1: *Data association accuracies*

(a) Kinematic only

Sensor	Track	% Correct	% Incorrect	% Missed
SSR	1	86	13	1
	2	85	13	2
ES	1	58	42	0
	2	57	41	2

(b) Joint kinematic and attribute

Sensor	Track	% Correct	% Incorrect	% Missed
SSR	1	99	0·5	0·5
	2	98	0·5	1·5
ES	1	71	28	1
	2	71	27	2

using the algorithm presented by Krieg [2002]. The performance of the state estimation algorithms is deferred to Section 5.3.

The measurement-to-target association is performed in two steps. In the first, probabilistic gating is used to eliminate the associations with a low probability of being correct. The constrained association algorithm, as described in Section 4.2, performs the second association step, that is, determining which of the remaining measurements are associated with each track. A *Monte Carlo* analysis is presented for two cases, namely association using only kinematic measurements, and association using both kinematic and attribute measurements.

For the case of kinematic only association, a significant number of the *Monte Carlo* runs result in the tracks swapping targets near the intersection of the two target trajectories. Such a run is presented in Figure 6(a), where the '+' and '∘' represent the SSR measurements from different targets—the ES measurements are not presented in the interest of picture clarity. On the other hand, the joint kinematic and attribute association algorithm successfully traverses both targets in all the runs, as illustrated in the single run of Figure 6(b).

The percentages of correct, incorrect and missed associations for both tracks under each algorithm are presented in Tables 1(a) and 1(b). The missed associations are a result of the probabilistic gating that precedes the association algorithm. As demonstrated by the results in the tables, the use of the attribute data for data association increases the degrees of discrimination available to the algorithm, resulting in an increase from around 85% correct association to 99% for the SSR data for this scenario. The gains are similar for the association of the ES data; the percentage of correct associations rises from below 60% for kinematic only association to just above 70% for joint kinematic and attribute association. The lower association accuracy for the ES data is an artifact of the relatively inaccurate bearing measurements and the lack of range discrimination of the ES sensor.

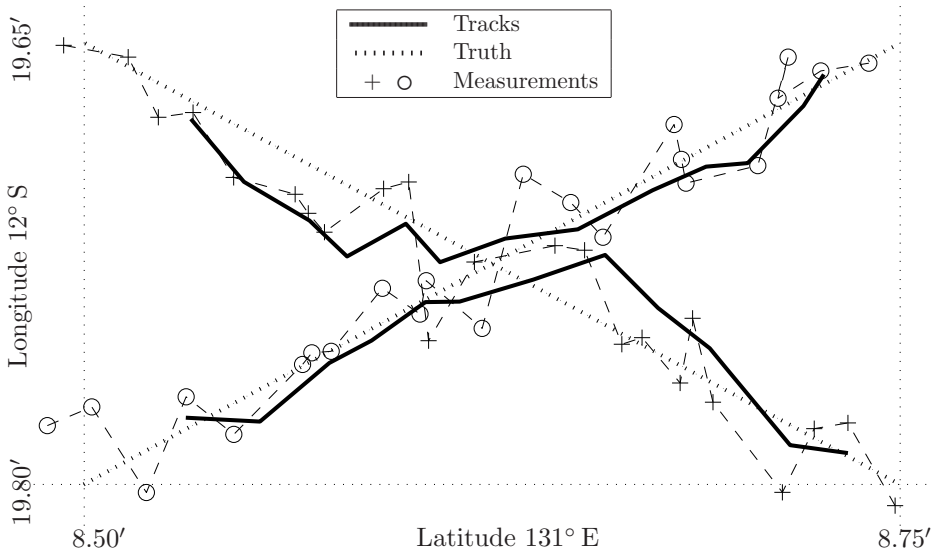

(a) Kinematic only

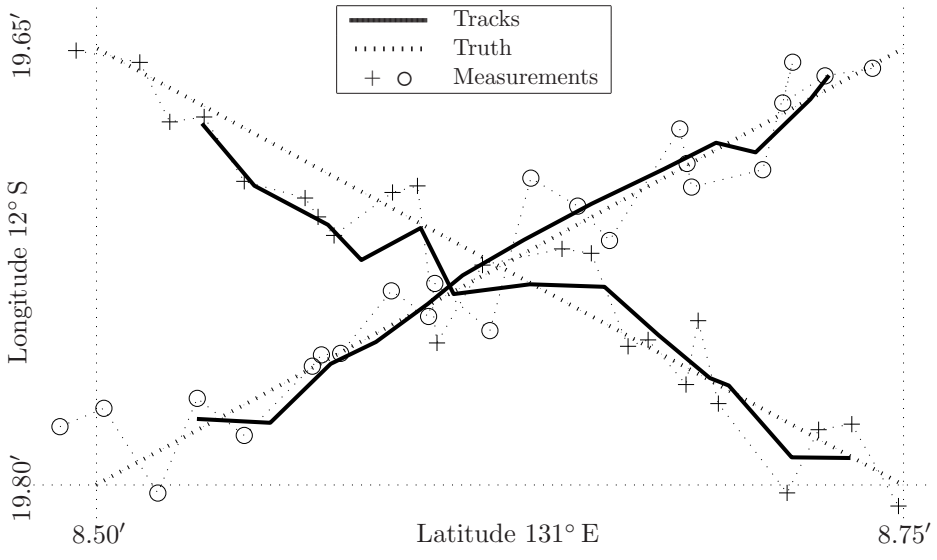

(b) Kinematic and attribute

Figure 6: *Track location with constrained association*

Table 2: *Identity estimation performance for kinematic and joint data association*

Track	Threshold	First exceeds		Exceeds	
		Kinematic	Joint	Kinematic	Joint
1	0.70	1	1	92 %	92 %
	0.75	5	5	87 %	87 %
	0.80	7	7	85 %	85 %
	0.85	7	7	85 %	82 %
	0.90	7	9	70 %	80 %
	0.95	9	9	53 %	80 %
2	0.70	1	1	97 %	97 %
	0.75	3	3	95 %	95 %
	0.80	3	3	95 %	95 %
	0.85	3	3	95 %	92 %
	0.90	5	5	87 %	90 %
	0.95	5	5	68 %	87 %

The majority of incorrect associations occur when the targets are in close proximity and following a track swap event.

Although this example demonstrates increased data association accuracy for the joint kinematic and attribute association over the kinematic only association, the magnitude of this increase is scenario dependent. For example, Khosla & Chen [2003] considered the inclusion of feature information in Dempster-Shafer and Probabilistic Argumentation System (PAS) association algorithms. They compared the kinematic and kinematic plus feature association using a more difficult three target scenario where the targets were on the limits of the sensor resolution for a significant period, and achieved a probability of 77% correct association for kinematic only association, and 98% correct association when using both kinematic and feature information. The greater difficulty inherent in their scenario is manifest in the lower performance for kinematic only association, but the similar performance when feature information is introduced indicates that greater benefit may be realised from the more difficult scenarios. That is, little benefit is expected for well separated targets, where the simplest of association algorithms will provide adequate performance, but the attribute data may be the difference between adequate and inadequate performance in dense target scenarios where the association gates of the tracks overlap.

The effect of kinematic only and joint kinematic and attribute data association on the identification probabilities obtained from multiple *Monte Carlo* runs are presented in Figures 7 and 8, respectively. Table 2 contains a comparative summary of the performance of the algorithm in terms of the number of the scan at which the identification probability first exceeds a particular threshold and the total percentage of scans for which the threshold is exceeded, averaged over all the runs. The results are presented for a range of probability thresholds from 0.7 to 0.95.

It is evident that the initial performance is almost identical for both association algorithms, as indicated by the figures and the *First exceeds* columns of Table 2. This is expected, as the two targets are well separated and easily discriminated during this period. However, the identification probabilities for the kinematic only association falls below that

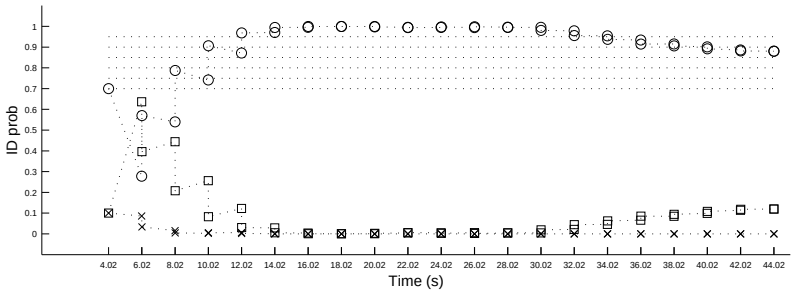

(a) Track 1

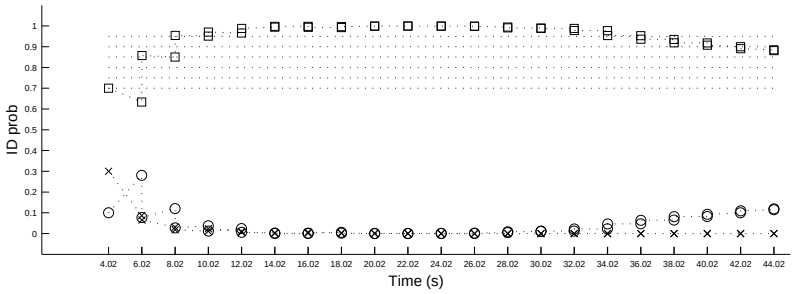

(b) Track 2

Figure 7: *Identification probabilities using kinematic only association*

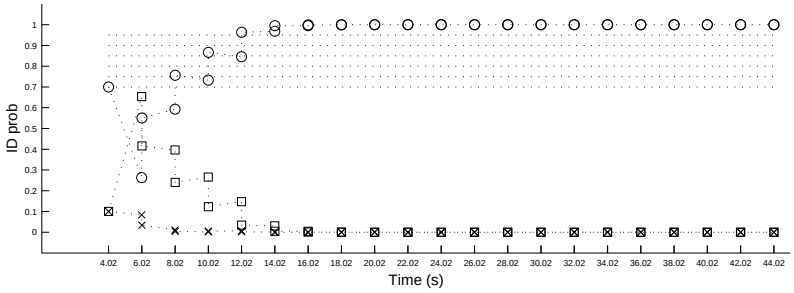

(a) Track 1

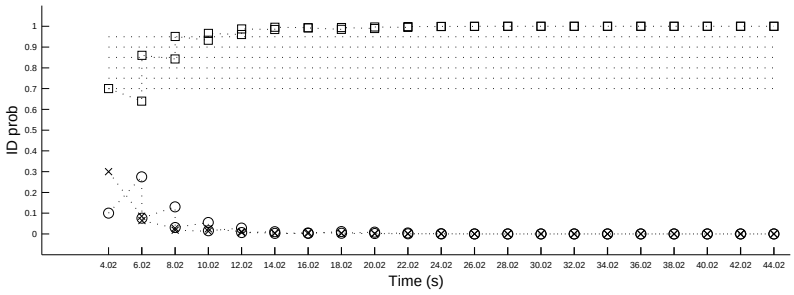

(b) Track 2

Figure 8: *Identification probabilities using joint kinematic and attribute association*

of the joint for the higher thresholds, as shown in the *Exceeds* columns of Table 2. This is supported by the falling probability for the correct identities in Figure 7, caused by the higher number of incorrect associations for the kinematic only association that result from the tracks swapping targets.

5 State Update

State estimation, or state update, problems may also be modelled by BBNs. The state or states of interest are represented by the hypothesis nodes of the BBN, and the measurements by the evidence nodes. The BBN grows over time: in the case of static or *non-evolutionary* state variables, evidence nodes are added as new measurements become available; and for dynamic or *evolutionary* state variables, evidence nodes and hypothesis nodes (representing the new or updated states of the variables at the time of the measurement) are added when new measurements become available.

Solutions are developed and demonstrated using a simulated target tracking and recognition application for both evolutionary and non-evolutionary state variable estimation.

5.1 Evolutionary State Update

The evolutionary states, that is, the states that change value over time, include both continuous and discrete state variables. In tracking applications, the most commonly occurring continuous evolutionary state variables are the kinematic states of a target, that is, position, velocity and, possibly, acceleration. Discrete evolutionary states may include variables such as the target flight level and weapon status.

The evolutionary state variables are handled by treating the time varying variable as a sequence of time invariant variables at specific times of interest, such as the measurement times. By way of an example, consider a time varying state variable X, and a set of measurements up to and including time t, that is, $Z^t \equiv \{Z_1, \ldots, Z_t\}$. Initially the BBN will consist solely of the node X_0, which represents the state of the variable X at a time instant prior to the arrival of any measurements. At the time of each measurement, two new nodes are added to the BBN, one representing the state of the variable at that measurement time and the other the measurement. This gives rise to the recursive structure of the BBN illustrated in Figure 9. The conditional probability $\mathtt{p}(x_t|x_{t-1})$ describes the evolution of the state of the variable X from time $t-1$ to t, and $\mathtt{p}(z_t|x_t)$, the likelihood of the measurement $Z_t = z_t$ given that the value of X is x.

The addition of new nodes will cause the network to grow over time. However, the objective is to estimate the state of X at some time t, based on the evidence or measurements up to and including that time. As such, it is not necessary to update the belief of the state of the nodes at times prior to t. Therefore the size of the network may be contained by making the node X_{t-1} a root node with prior probability $\mathtt{p}\left(x_{t-1}|Z^{t-1}\right)$, and removing all other nodes at times up to and including $t-1$.

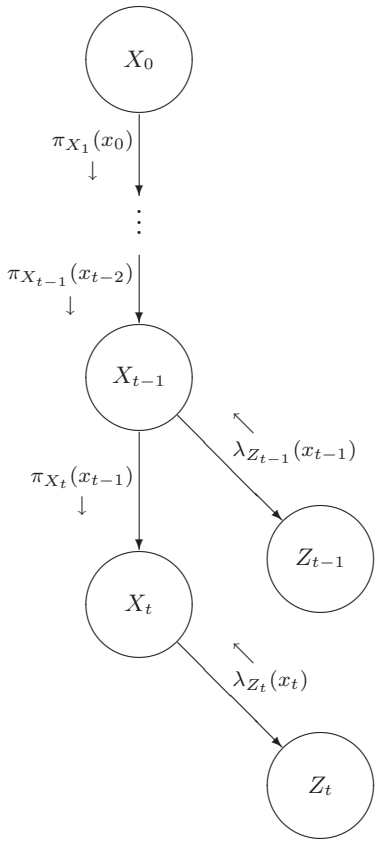

Figure 9: *A BBN for updating evolutionary state variables*

Consider the BBN of Figure 9, and let $\text{Bel}_{t'}(x_t)$ be the posterior probability, or belief, that $X_t = x_t$, given all the measurements up to and including the time t'. The belief that $X_0 = x_0$ at time 0 is the prior probability of x, that is,

$$\text{Bel}_0(x_0) = \mathtt{p}\,(x_0)\,. \tag{27}$$

Then, at each recursion, the belief at the new state node becomes

$$\text{Bel}_t(x_t) \equiv \mathtt{p}\left(x_t|Z^t\right) = \alpha_t \lambda_t(x_t)\pi_t(x_t), \tag{28}$$

where α_t is a normalising constant at time t. Given $\lambda(z_t) = \delta_{z_t z'_t}$ and using (2), the retrospective support may be written as

$$\lambda_t(x_t) = \int_z \mathtt{p}\,(z|x_t)\,\lambda(z_t)\,dz = \mathtt{p}\left(z'_t|x_t\right). \tag{29}$$

The predictive support, $\pi_t(x_t)$, represents the prior knowledge of the state at the time t given the prior knowledge of the state at time 0 and all the evidence or measurements up to the time t. Using (5), (6) and (1), the predictive support becomes

$$\pi_t(x_t) = \int_{x_{t-1}} \mathrm{p}\left(x_t|x_{t-1}\right) \pi_{X_t}(x_{t-1}) dx_{t-1} \tag{30}$$

$$= \int_{x_{t-1}} \mathrm{p}\left(x_t|x_{t-1}\right) \lambda_{Z_{t-1}}(x_{t-1}) \pi(x_{t-1}) dx_{t-1} \tag{31}$$

$$= \int_{x_{t-1}} \mathrm{p}\left(x_t|x_{t-1}\right) \mathrm{Bel}_{t-1}(x_{t-1})\, dx_{t-1}. \tag{32}$$

Strictly speaking, $\mathrm{Bel}_{t-1}(x_{t-1}) = \alpha_{t-1}\lambda_{Z_{t-1}}(x_{t-1})\pi(x_{t-1})$, but the normalising constant α_{t-1} is absorbed by the new normalising constant α_t and is omitted here. The belief that $X_t = x_t$ then becomes

$$\mathrm{Bel}_t(x_t) = \alpha_t \mathrm{p}\left(z'_t|x_t\right) \int_{x_{t-1}} \mathrm{p}\left(x_t|x_{t-1}\right) \mathrm{Bel}_{t-1}(x_{t-1})\, dx_{t-1} \tag{33}$$

or, in terms of the posterior probabilities,

$$\mathrm{p}\left(x_t|Z^t\right) = \alpha_t \mathrm{p}\left(z'_t|x_t\right) \int_{x_{t-1}} \mathrm{p}\left(x_t|x_{t-1}\right) \mathrm{p}\left(x_{t-1}|Z^{t-1}\right) dx_{t-1}. \tag{34}$$

The normalising constant α_t may be dropped because the estimate of x_t is found by maximising (33), that is,

$$\hat{x}_t = \arg\max_{x_t}(\mathrm{Bel}_t(x_t)). \tag{35}$$

The tracking problem is one of obtaining the best state estimate at the current time. Therefore, it is not necessary to update the beliefs of the state variable at times other than t. The solution for the special case of continuous variables, for example, kinematic states, for linear and Gaussian systems may be obtained by applying the Kalman filter to the measurements. This result may also be applied to the estimation of discrete variables by replacing the integrals with summations. Track *smoothing* algorithms, which form estimates of the state variables using both the past and future measurements, may be developed by calculating $\mathrm{Bel}_{t'}(x_t)$ for all $t \leq t'$ from the BBN in Figure 9.

5.2 Non-Evolutionary State Update

A non-evolutionary variable is represented by a single node in a BBN, as its value does not change over time. The BBN for this class of problem is also dynamic, as new measurement nodes are added to the network at each measurement time. The target recognition problem, that is, target type and identity (ID) estimation, is used here to illustrate the development of a solution to the problem of estimating non-evolutionary state variables.

Consider the BBN of Figure 10, which models the dependencies between the target class state variable C, identity state variable I, Secondary Surveillance Radar (SSR)

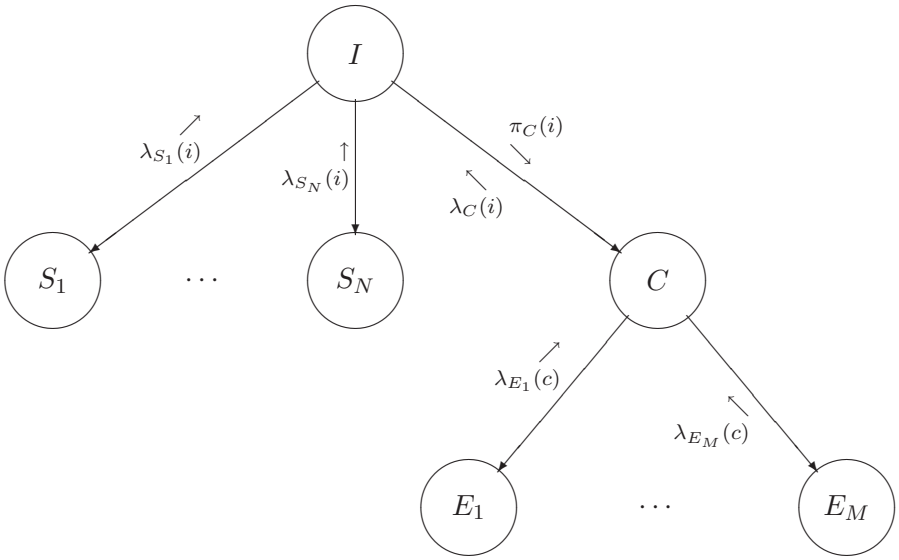

Figure 10: *A non-evolutionary BBN for target identification and classification*

measurements S_n, $n = 1, \ldots, N$, and Electronic Surveillance (ES) measurements E_m, $m = 1, \ldots, M$. Although the SSR and ES measurements are not required to occur simultaneously, the dependency between class and identity dictates that both are updated on receipt of either an ES or SSR measurement. The choice of whether the class is dependent on the identity, or vice versa, is arbitrary. In this example, it is assumed that the number of each type of platform, that is, the probability of each, is determined by the relevant nation or force, hence the dependency of class on identity.

The special case of discrete variables is presented here as both class and identity take discrete values, and only the discrete target identity and class measurements are considered from the SSR and ES sensors, respectively; the kinematic measurements are ignored for the purpose of this treatment. The generalisation to the continuous domain is achieved by replacing the summations with integrals in the following.

For the example of Figure 10, denote s'_n and e'_m as the measured values from the SSR and ES, respectively. Then using (1) through (6) and $\pi(i) = \mathtt{p}(i)$, the belief in the proposition $I = i$ is

$$\begin{aligned} \mathrm{Bel}(i) &= \alpha\lambda(i)\pi(i) \\ &= \alpha\lambda_C(i)\prod_{n=1}^{N}\lambda_{S_n}(i)\mathtt{p}(i) \\ &= \alpha\,\mathtt{p}(i)\prod_{n=1}^{N}\mathtt{p}(s_n|i)\sum_c \mathtt{p}(c|i)\prod_{m=1}^{M}\mathtt{p}(e_m|c)\,. \end{aligned} \tag{36}$$

Similarly, the posterior probability that $C = c$ is written

$$\text{Bel}(c) = \alpha \prod_{m=1}^{M} \mathtt{p}\left(e_m|c\right) \sum_i \mathtt{p}\left(c|i\right) \mathtt{p}\left(i\right) \prod_{n=1}^{N} \mathtt{p}\left(s_n|i\right). \tag{37}$$

Prior to any measurements, (36) and (37) reduce to the prior probabilities of I and C, namely

$$\text{Bel}(i) = \mathtt{p}\left(i\right), \text{ and} \tag{38}$$

$$\text{Bel}(c) = \sum_i \mathtt{p}\left(c|i\right) \mathtt{p}\left(i\right). \tag{39}$$

As the measurements are added to the BBN, (36) and (37) are recalculated to give the latest posterior probabilities.

The solution is not recursive in its current form. However, the following outlines a partially recursive solution. Defining

$$\begin{aligned} \mathtt{p}\left(S^0|i\right) &= 1, \text{ and} \\ \mathtt{p}\left(E^0|c\right) &= 1, \end{aligned} \tag{40}$$

the recursive conditional measurement probabilities are defined as

$$\mathtt{p}\left(S^n|i\right) = \mathtt{p}\left(S^{n-1}|i\right) \mathtt{p}\left(s_n|i\right), \text{ and} \tag{41}$$

$$\mathtt{p}\left(E^m|c\right) = \mathtt{p}\left(E^{m-1}|c\right) \mathtt{p}\left(e_m|c\right), \tag{42}$$

for all the values of i and c. Based on these definitions, the beliefs (36) and (37) become

$$\text{Bel}(i) = \alpha\, \mathtt{p}\left(i\right) \mathtt{p}\left(S^n|i\right) \sum_c \mathtt{p}\left(c|i\right) \mathtt{p}\left(E^m|c\right), \text{ and} \tag{43}$$

$$\text{Bel}(c) = \alpha \mathtt{p}\left(E^m|c\right) \sum_i \mathtt{p}\left(c|i\right) \mathtt{p}\left(i\right) \mathtt{p}\left(S^n|i\right). \tag{44}$$

The solution is then found by recursively updating the conditional measurement probabilities, which are then used to recalculate the identity and class beliefs.

The BBN in Figure 10 may be extended to include other sources of identity and class measurements, such as target dynamics and non-cooperative target recognition. Additional state variables, such as category (air, surface, subsurface, land, and space), may also be added to the BBN model.

5.3 Simulation Results

The crossing target scenario of Section 4.3 is used here to demonstrate the state estimation algorithms. Again SSR and ES sensor measurements are simulated. The simulated SSR measurement errors have a standard deviation of 0.5° and 20 m for bearing and range, respectively. The SSR also returns an identity from the set $\{1, 2, 3\}$, with a probability of 0.7 that the correct identity of 1 is received from Target 1, and a probability of 0.7 that the correct identity of 2 is received from Target 2. The standard deviation of the errors from

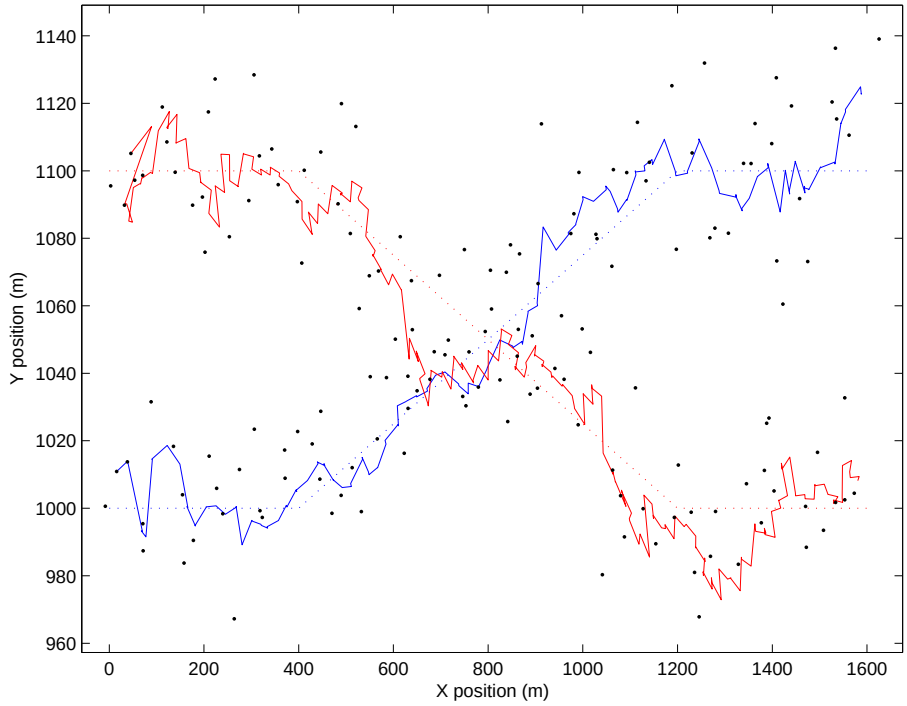

Figure 11: *SSR measurements and track positions for the crossing target scenario*

the ES sensor is 2°, and the sensor returns a platform class from the set $\{1, 2, 3, 4\}$ with a probability of 0.7 that the correct class of 1 is received from Target 1, and a probability of 0.7 that the correct class of 3 is received from Target 2. The remaining values for the identity and class measurements occur equi-likely. A single measurement is generated for each target from both sensors simultaneously at one second intervals.

As data association is a necessary precursor to state estimation, the simulated measurements are input to the constrained data association algorithm of Section 4, which uses both kinematic and attribute data to associate the measurements to the tracks. (The performance of the data association algorithm was analysed in Section 4.3 and is not directly analysed here. However it is acknowledged that it will influence the performance of the state estimation algorithms.) The associated measurements are then processed by the state estimation algorithms, that is, the Kalman filter (Section 5.1) to update the kinematic states, and the non-evolutionary state estimation algorithm of Section 5.2 to update the identity and class of the targets. The kinematic state estimation and attribute (target class) state estimation algorithms are processed independently, with each estimating different target state variables using different sets of measurements. Both tracking and data association are performed in polar coordinates.

The track positions from a single simulation run are presented in Cartesian coordinates in Figure 11, where the solid lines represent the tracks, the dotted lines the true target trajectories, and the dots the SSR measurements. In almost all the runs, the tracks correctly follow the crossing targets. The ability to accurately estimate the identity and class of the targets improves the data association performance, and hence the kinematic

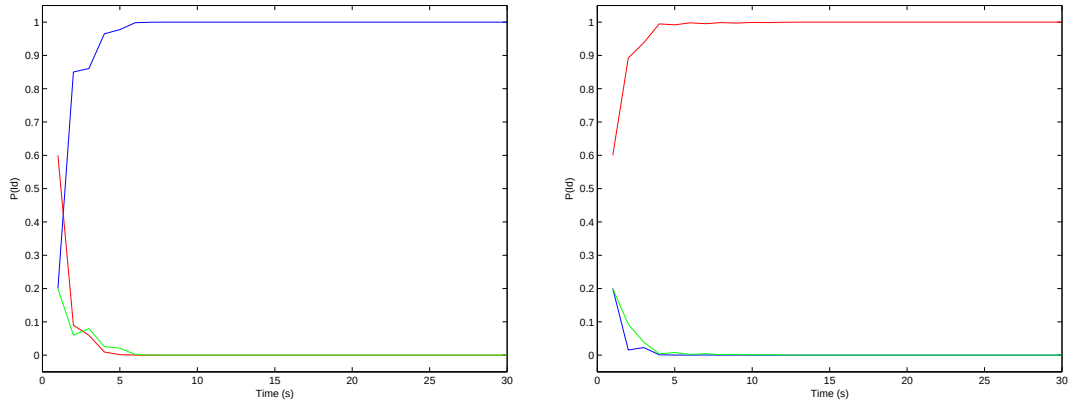

(a) Track 1 *(b) Track 2*

Figure 12: *Identity probabilities for the crossing target scenario*

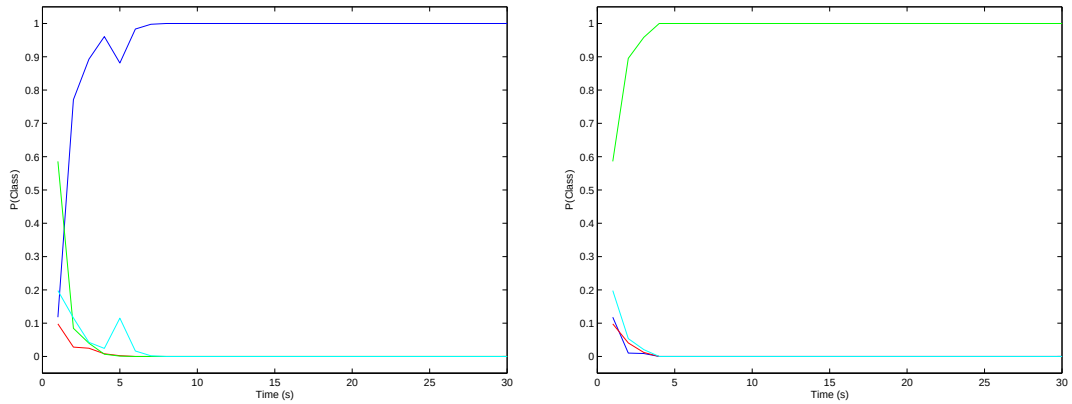

(a) Track 1 *(b) Track 2*

Figure 13: *Class probabilities for the crossing target scenario*

tracking performance. The figures 12(a) and 12(b) show the estimated probabilities for each of the possible identities over the first 30 seconds for tracks 1 and 2, respectively. The blue, red and green lines represent the probabilities for identities 1, 2 and 3, respectively. Within a few measurement updates, the probability of identity 1 for Track 1 correctly approaches unity. Likewise, the probability of identity 2 for track 2 also approaches unity within the receipt of a few measurements. The presence of subsequent conflicting, or incorrect, identity measurements reduce these probabilities, particularly early in the scenario where fewer measurements contribute to the identity estimation. This effect is evident in Figure 12(a), where an erroneous identity 3 measurement at three seconds increases the probability of identity 3. The lessening effect of conflicting measurements as more correct measurements are received is illustrated by the near constant identity probabilities after ten seconds.

The Figures 13(a) and 13(b) present the probabilities for each of the possible classes over the first 30 seconds for both tracks 1 and 2, with the blue, red, green and cyan lines representing the probabilities for classes 1, 2, 3 and 4, respectively. Within several measurement scans, the probability of Class 1 correctly approaches unity for Track 1, and the probability of Class 3 approaches unity for Track 2. As for the identity, the effect of erroneous measurements shortly after track initiation is again illustrated, where an incorrect class 4 measurement at five seconds increases the probability of Class 4 and decreases the probability of Class 1 for Track 1, as shown in Figure 13(a). In addition, because of the dependency between class and identity, incorrect identity measurements influence the class probabilities and incorrect class measurements influence the identity probabilities.

6 Joint Tracking and Classification

Consider an example tracking and recognition application where the class and kinematic states of an object are estimated from inaccurate class and kinematic measurements. This problem may be represented by the BBN in Figure 14, where the variable C represents the (time invariant) target class, X_k the kinematic state at time k, Z_k the target kinematic measurement at time k, and S_k the class measurement at time k. The BBN grows over time, with the addition of new X, Z and S nodes at each time step. This growth at each time step provides a framework for developing a recursive algorithm.

The BBN of Figure 14 contains loops in the underlying Markov network; therefore it requires an iterative algorithm to obtain a solution, to which it may or may not converge. As for previous cases, this problem is overcome by aggregating interconnected groups of variables into composite variables or clusters [Pearl 1988, Krieg 2001]. An equivalent clustered BBN is presented in Figure 15, where

$$\begin{aligned} Y_0 &= \{X_0, C\}\,, \\ Y_k &= \{X_k, X_{k-1}, C\} \qquad k \geq 1, \\ A_k &= \{S_k, C\} \qquad k \geq 1, \\ B_k &= \{Z_k, X_k\} \qquad k \geq 1. \end{aligned} \tag{45}$$

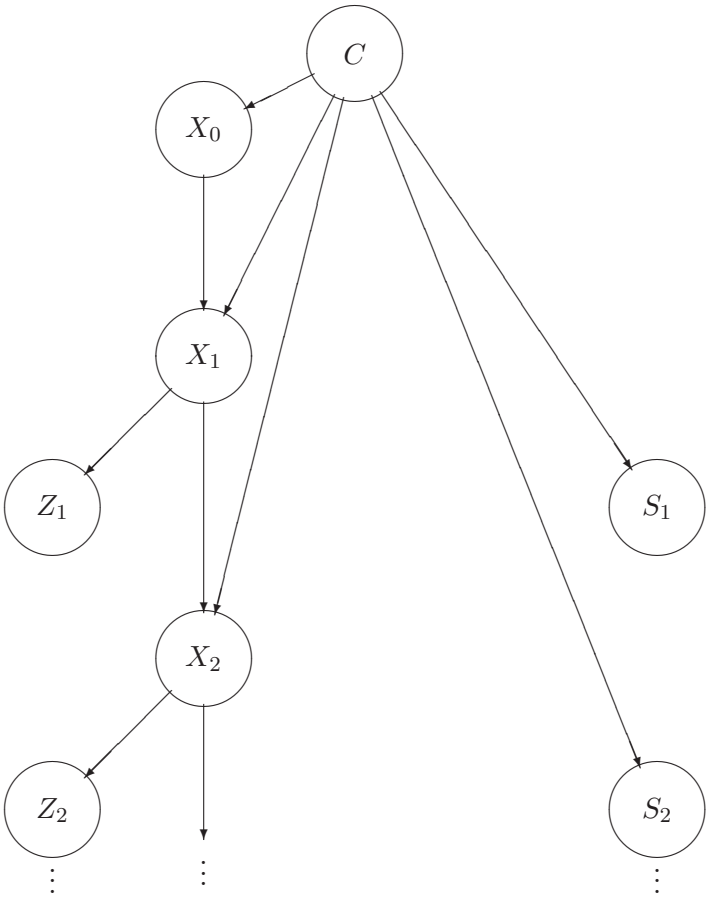

Figure 14: *BBN representation of a joint tracking and classification problem*

The conditional probabilities associated with each link between the composite nodes are the joint probability of all the variables in the child composite node conditioned on all the variables common to both nodes connected by the link, that is,

$$\begin{aligned} \mathtt{p}\left(y_k|y_{k-1}\right) &= \mathtt{p}\left(x_k, x_{k-1}, c|x_{k-1}, c\right) = \mathtt{p}\left(x_k|x_{k-1}, c\right), \\ \mathtt{p}\left(a_k|y_k\right) &= \mathtt{p}\left(s_k, c|c\right) = \mathtt{p}\left(s_k|c\right), \\ \mathtt{p}\left(b_k|y_k\right) &= \mathtt{p}\left(z_k, x_k|x_k\right) = \mathtt{p}\left(z_k|x_k\right). \end{aligned} \tag{46}$$

The clustered BBN is capable of representing states containing various kinematic and attribute data, where the attributes may include any of target identity, category and class. In general, the composite variable A_k represents all measurements relating to time invariant parameters, and B_k those relating to time varying parameters. The variables of interest are obtained by marginalising the composite state variables.

Based on this generality, the approach here is to initially solve for the composite state variables Y_k, $k = 0, 1, 2, \ldots$. As the belief is a posterior probability, the belief that the state variable $Y_k = y_k$, given all measurements up to time k, is denoted $\mathtt{p}\left(y_k|A^k, B^k\right)$.

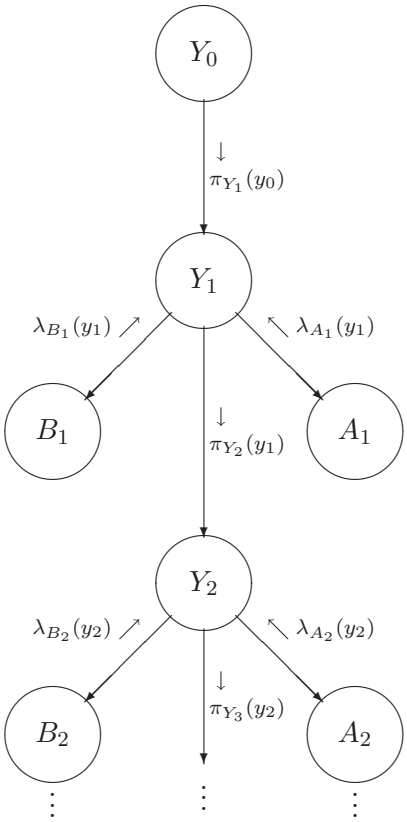

Figure 15: *Equivalent clustered BBN for joint tracking and classification*

At the time 0, the BBN contains the single variable Y_0, with prior probability $\mathtt{p}(y_0) \equiv \mathtt{p}\left(y_0|A^0, B^0\right)$, where A^0 and B^0 are the (empty) sets of measurements up to time 0. Using Figure 14 and equation (45), the prior probability of $Y_0 = y_0$ is

$$\mathtt{p}(y_0) = \mathtt{p}(x_0|c)\,\mathtt{p}(c)\,. \tag{47}$$

Now, consider an arbitrary time k, where the BBN terminates with nodes Y_k, A_k and B_k. From (1) and (3), the belief, $\mathtt{p}\left(y_k|A^k, B^k\right)$, is the normalised product of $\pi(y_k)$, $\lambda_{A_k}(y_k)$ and $\lambda_{B_k}(y_k)$. Assuming that A_k only contains instantiated leaf or measurement nodes, and nodes common to both itself and Y_k, the value of A_k is denoted a'_k, and $\lambda(a_k) = \delta_{a_k a'_k}$, which equals 1 if $a_k = a'_k$ and zero otherwise. Therefore, using (4),

$$\begin{aligned} \lambda_{A_k}(y_k) &= \int_{a_k} \mathtt{p}(a_k|y_k)\,\lambda(a_k)\,da_k \\ &= \mathtt{p}\left(a'_k|y_k\right). \end{aligned} \tag{48}$$

Similarly,

$$\lambda_{B_k}(y_k) = \mathtt{p}\left(b'_k|y_k\right). \tag{49}$$

Assuming $\pi_{Y_k}(y_{k-1})$ is known, (5) gives

$$\pi(y_k) = \int_{y_{k-1}} \mathtt{p}(y_k|y_{k-1})\,\pi_{Y_k}(y_{k-1})\,dy_{k-1}, \tag{50}$$

and

$$\mathtt{p}\left(y_k|A^k,B^k\right) \equiv \mathrm{Bel}_k(y_k) = \alpha_k \mathtt{p}\left(a'_k|y_k\right)\mathtt{p}\left(b'_k|y_k\right)\int\limits_{y_{k-1}} \mathtt{p}\left(y_k|y_{k-1}\right)\pi_{Y_k}(y_{k-1})\,dy_{k-1}. \quad (51)$$

Adding another variable Y_{k+1} to the BBN, that is, the state at time $k+1$, (6) provides

$$\begin{aligned}\pi_{Y_{k+1}}(y_k) &= \mathtt{p}\left(a'_k|y_k\right)\mathtt{p}\left(b'_k|y_k\right)\int\limits_{y_{k-1}} \mathtt{p}\left(y_k|y_{k-1}\right)\pi_{Y_k}(y_{k-1})\,dy_{k-1} \\ &= \alpha_k^{-1}\mathtt{p}\left(y_k|A^k,B^k\right).\end{aligned} \quad (52)$$

Therefore, $\pi_{Y_k}(y_{k-1}) = \alpha_{k-1}^{-1}\mathtt{p}\left(y_{k-1}|A^{k-1},B^{k-1}\right)$, and (51) becomes

$$\mathtt{p}\left(y_k|A^k,B^k\right) = \alpha_k \mathtt{p}\left(a'_k|y_k\right)\mathtt{p}\left(b'_k|y_k\right)\alpha_{k-1}^{-1}\int\limits_{y_{k-1}} \mathtt{p}\left(y_k|y_{k-1}\right)\mathtt{p}\left(y_{k-1}|A^{k-1},B^{k-1}\right)dy_{k-1}, \quad (53)$$

where

$$\alpha_k = \left(\int\limits_{y_k}\mathtt{p}\left(a'_k|y_k\right)\mathtt{p}\left(b'_k|y_k\right)\alpha_{k-1}^{-1}\int\limits_{y_{k-1}}\mathtt{p}\left(y_k|y_{k-1}\right)\mathtt{p}\left(y_{k-1}|A^{k-1},B^{k-1}\right)dy_{k-1}dy_k\right)^{-1}. \quad (54)$$

Substituting the definitions of (45) and the probabilities of (46), and absorbing the constant α_{k-1}^{-1} into α_k, the posterior probability (53) becomes, in terms of the original variables,

$$\begin{aligned}\mathtt{p}\left(x_k,x_{k-1},c|Z^k,S^k\right) &= \alpha_k \mathtt{p}\left(s'_k|c\right)\mathtt{p}\left(z'_k|x_k\right)\mathtt{p}\left(x_k|x_{k-1},c\right) \\ &\quad\times\int\limits_{x_{k-2}}\mathtt{p}\left(x_{k-1},x_{k-2},c|Z^{k-1},S^{k-1}\right)dx_{k-2} \\ &= \alpha_k \mathtt{p}\left(s'_k|c\right)\mathtt{p}\left(z'_k|x_k\right)\mathtt{p}\left(x_k|x_{k-1},c\right)\mathtt{p}\left(x_{k-1},c|Z^{k-1},S^{k-1}\right).\end{aligned} \quad (55)$$

Integrating over x_{k-1} gives

$$\begin{aligned}\mathtt{p}\left(x_k,c|Z^k,S^k\right) &= \alpha_k \mathtt{p}\left(s'_k|c\right)\mathtt{p}\left(z'_k|x_k\right) \\ &\quad\times\int\limits_{x_{k-1}}\mathtt{p}\left(x_k|x_{k-1},c\right)\mathtt{p}\left(x_{k-1},c|Z^{k-1},S^{k-1}\right)dx_{k-1} \\ &= \alpha_k \mathtt{p}\left(s'_k|c\right)\mathtt{p}\left(c|Z^{k-1},S^{k-1}\right)\mathtt{p}\left(z'_k|x_k\right) \\ &\quad\times\int\limits_{x_{k-1}}\mathtt{p}\left(x_k|x_{k-1},c\right)\mathtt{p}\left(x_{k-1}|c,Z^{k-1},S^{k-1}\right)dx_{k-1}.\end{aligned} \quad (56)$$

From Bayes Rule,

$$\begin{aligned}&\mathtt{p}\left(z_k|x_k\right)\int\limits_{x_{k-1}}\mathtt{p}\left(x_k|x_{k-1},c\right)\mathtt{p}\left(x_{k-1}|c,Z^{k-1},S^{k-1}\right)dx_{k-1} \\ &\equiv \mathtt{p}\left(x_k|c,Z^k,S^{k-1}\right)\beta_k^{(c)},\end{aligned} \quad (57)$$

where

$$\beta_k^{(c)} = \int_{x_k} \mathtt{p}\left(z_k|x_k\right) \int_{x_{k-1}} \mathtt{p}\left(x_k|x_{k-1},c\right) \mathtt{p}\left(x_{k-1}|c,Z^{k-1},S^{k-1}\right) dx_{k-1}\, dx_k. \tag{58}$$

Similarly,

$$\begin{aligned} &\mathtt{p}\left(s_k'|c\right) \mathtt{p}\left(c|Z^{k-1},S^{k-1}\right) \\ &\equiv \mathtt{p}\left(c|Z^{k-1},S^{k}\right) \gamma_k, \end{aligned} \tag{59}$$

where

$$\gamma_k = \sum_c \mathtt{p}\left(s_k'|c\right) \mathtt{p}\left(c|Z^{k-1},S^{k-1}\right). \tag{60}$$

Substituting (57) and (59) into (56) gives

$$\mathtt{p}\left(x_k,c|Z^k,S^k\right) = \gamma_k \mathtt{p}\left(c|Z^{k-1},S^k\right) \beta_k^{(c)} \mathtt{p}\left(x_k|c,Z^k,S^{k-1}\right), \tag{61}$$

where

$$\mathtt{p}\left(x_k|c,Z^k,S^{k-1}\right) = \beta_k^{(c)-1} \mathtt{p}\left(z_k|x_k\right) \int_{x_{k-1}} \mathtt{p}\left(x_k|x_{k-1},c\right) \mathtt{p}\left(x_{k-1}|c,Z^{k-1},S^{k-1}\right) dx_{k-1}, \tag{62}$$

$$\mathtt{p}\left(c|Z^{k-1},S^k\right) = \gamma_k^{-1} \mathtt{p}\left(s_k'|c\right) \mathtt{p}\left(c|Z^{k-1},S^{k-1}\right), \tag{63}$$

and $\beta_k^{(c)}$ and γ_k are defined in (58) and (60), respectively.

The class given all the class and kinematic measurements is obtained by integrating (61) over all values of x_k, that is,

$$\begin{aligned} \mathtt{p}\left(c|Z^k,S^k\right) &= \gamma_k \mathtt{p}\left(c|Z^{k-1},S^k\right) \beta_k^{(c)} \int_{x_k} \mathtt{p}\left(x_k|c,Z^k,S^{k-1}\right) dx_k \\ &= \gamma_k \mathtt{p}\left(c|Z^{k-1},S^k\right) \beta_k^{(c)}. \end{aligned} \tag{64}$$

Similarly, the kinematic state given all the kinematic and class measurements is now obtained by summing (61) over all values of c, that is,

$$\begin{aligned} \mathtt{p}\left(x_k|Z^k,S^k\right) &= \gamma_k \sum_c \mathtt{p}\left(c|Z^{k-1},S^k\right) \beta_k^{(c)} \mathtt{p}\left(x_k|c,Z^k,S^{k-1}\right) \\ &= \sum_c \mathtt{p}\left(c|Z^k,S^k\right) \mathtt{p}\left(x_k|c,Z^k,S^{k-1}\right). \end{aligned} \tag{65}$$

Therefore the probabilities $\mathtt{p}\left(x_k|c,Z^k,S^{k-1}\right)$ and $\mathtt{p}\left(c|Z^{k-1},S^k\right)$ may be recursively estimated at each time step using equations (62) and (63), and the prior probabilities

$$\mathtt{p}\left(x_0|c,Z^0,S^0\right) \equiv \mathtt{p}\left(x_0|c\right), \text{ and} \tag{66}$$

$$\mathtt{p}\left(c|Z^0,S^0\right) \equiv \mathtt{p}\left(c\right). \tag{67}$$

(Z^0 and S^0 denote the empty kinematic and attribute measurement sets at time 0.) From these, the posterior probabilities $\mathtt{p}\left(c|Z^k, S^k\right)$ and $\mathtt{p}\left(x_k, |Z^k, S^k\right)$ may be calculated at each time step using (64) and (65). These posterior probabilities are then used to obtain the most likely values for these variables.

This approach differs from that of Challa & Pulford [1999], which incorporates a time variant model for the target class that uses a transition matrix to define the probability that the target class will change. Although the target class does not change, in practice it may prove useful in allowing more rapid correction of incorrect classification decisions, or may assist in correcting tracking errors, such as track swaps.

6.1 Linear Gaussian Kinematic Systems

Linear Gaussian systems comprise a linear target motion model with white Gaussian additive noise, which, for the time interval $k-1$ to k, may be defined as

$$x_k = F_{k-1}x_{k-1} + w_{k-1}, \tag{68}$$

where F_{k-1} represents the state transition matrix and w_{k-1} is the zero mean process noise with covariance Q_{k-1}. The conditional probability $\mathtt{p}\left(x_k|x_{k-1}, c\right)$ is distributed as $\mathcal{N}\left(x_k : F_{k-1}^{(c)}x_{k-1}, Q_{k-1}^{(c)}\right)$, and the prior probability $\mathtt{p}\left(x_0\right)$ as $\mathcal{N}\left(x_0 : \bar{x}_0^{(c)}, P_0^{(c)}\right)$, where $\mathcal{N}\left(\cdot\right)$ denotes the normal or Gaussian distribution, and $^{(c)}$ denotes the class to which the model applies. Similarly, the linear Gaussian kinematic measurement model with white Gaussian additive noise for class c at time k is given by

$$z_k = H_k^{(c)}x_k^{(c)} + v_k^{(c)}, \tag{69}$$

where $H_k^{(c)}$ is the measurement matrix that maps the state space onto the measurement space, $v_k^{(c)}$ is the zero mean measurement noise with covariance $R_k^{(c)}$, and the conditional probability $\mathtt{p}\left(z_k|x_k\right)$ is distributed as $\mathcal{N}\left(z_k : H_k^{(c)}x_k^{(c)}, R_k^{(c)}\right)$. The attribute measurement model is a probability mass function representing the discrete measurement probabilities, given the state.

Substituting the Gaussian probabilities into (62) and (57), and rearranging, gives

$$\begin{aligned}\mathtt{p}\left(x_k|c, Z^k, S^{k-1}\right) &= \beta_k^{(c)-1}\mathcal{N}\left(z_k' : H_k^{(c)}x_k^{(c)}, R_k\right) \\ &\times \int_{x_{k-1}^{(c)}} \mathcal{N}\left(x_k^{(c)} : F_{k-1}^{(c)}x_{k-1}^{(c)}, Q_{k-1}^{(c)}\right)\mathcal{N}\left(x_{k-1}^{(c)} : \bar{x}_{k-1|k-1}^{(c)}, P_{k-1|k-1}^{(c)}\right)dx_{k-1}^{(c)},\end{aligned} \tag{70}$$

where $x_{i|j}^{(c)}$ and $P_{i|j}^{(c)}$ are the mean and covariance of the state estimate for model c at time i given all the measurements up to and including time j, and

$$\begin{aligned}\beta_k^{(c)} &= \int_{x_k^{(c)}} \mathcal{N}\left(z_k' : H_k^{(c)} x_k^{(c)}, R_k\right) \\ &\quad \times \int_{x_{k-1}^{(c)}} \mathcal{N}\left(x_k^{(c)} : F_{k-1}^{(c)} x_{k-1}^{(c)}, Q_{k-1}^{(c)}\right) \mathcal{N}\left(x_{k-1}^{(c)} : \bar{x}_{k-1|k-1}^{(c)}, P_{k-1|k-1}^{(c)}\right) dx_{k-1}^{(c)}\, dx_k^{(c)} \quad (71) \\ &= \mathcal{N}\left(z_k' : H_k^{(c)} \bar{x}_{k|k-1}^{(c)}, H_k^{(c)} P_{k+1|k}^{(c)} H_k^{(c)\,\mathrm{T}} + R_k\right).\end{aligned}$$

The solution to (70) may be obtained using a Kalman filter for each class, which may then be used in (65) and (64) to obtain the solutions for $\mathtt{p}\left(x_k|Z^k, S^k\right)$ and $\mathtt{p}\left(c|Z^k, S^k\right)$, respectively. In particular, $\mathtt{p}\left(x_k|Z^k, S^k\right)$ may be calculated using a multiple model Kalman filter, where the model probabilities are $\mathtt{p}\left(c|Z^k, S^k\right) = \gamma_k \mathtt{p}\left(c|Z^{k-1}, S^k\right) \beta_k^{(c)}$.

6.2 Simulation Results

A scenario with a single target that performs a $2\,g$ and a $0.5\,g$ turn is used to evaluate the joint tracking and classification algorithm. The target may take one of two possible classes, namely *C1*, which is a non-manoeuvring platform, and *C2*, which is capable of performing significant manoeuvres. The sensor *S1* provides bearing and range measurements and is representative of a primary radar, and sensor *S2* provides bearing and class measurements and is representative of an ES sensor. The class measurements of *S2* are correct 80% of the time. Sensor *S1* provides measurements at 1 Hz, and *S2* provides measurements at 0.2 Hz. The non-linear measurement function, which maps the polar coordinate sensor measurement space onto the Cartesian state space, is linearised using an EKF.

The estimated track position (solid line) and measurements (dots) from *S1* are shown in Figure 16, with the estimates from the constant velocity and manoeuvring models in Figures 17(a) and 17(b), respectively. These figures show that, after the first manoeuvre when the probability of class *C2* is almost unity, the kinematic state estimates from the manoeuvring model dominate the positional estimates. This is expected, as the class probabilities provide the summation weights for the multiple model kinematic tracker.

Figure 18 shows the estimated probability that the target is class *C2* over time. The probability increases with the number of class measurements over the first 20 s of the scenario, albeit with the occasional decrease in the probability caused by the 20% of class measurements that are incorrect. The first manoeuvre, which occurs after 20 s, reinforces class *C2*, significantly increasing its probability. The incorrect measurements now have less impact, particularly after the second manoeuvre at 40 s, which also supports the *C2* class.

To further understand the interaction between the kinematic and attribute measurements and states, the scenario is repeated with the class measurements supporting class *C1*, which is in direct conflict with the target dynamics employed in the scenario. This situation is artificial and should only occur in practice if the measurements are incorrectly

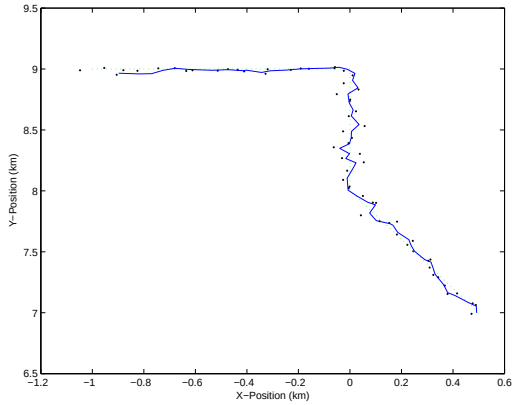

Figure 16: *Track position from position and class measurements*

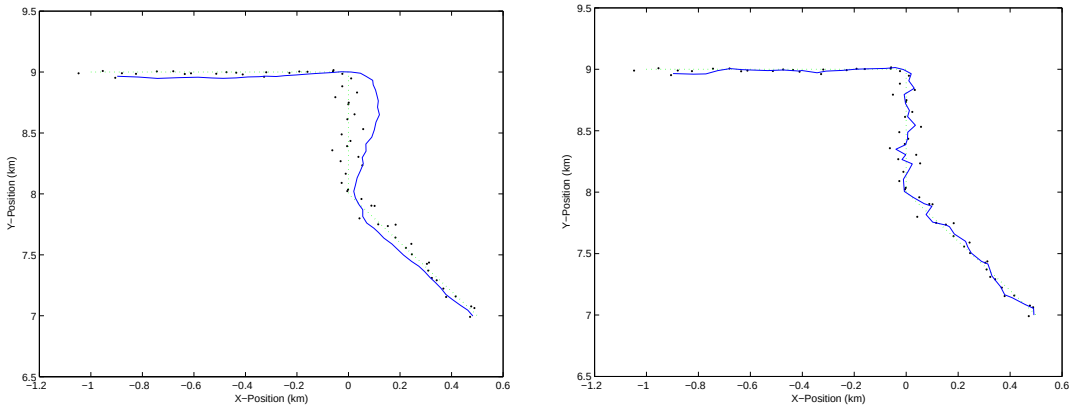

(a) Constant velocity model *(b) Manoeuvring model*

Figure 17: *Individual model track position from position and class measurements*

associated to the track; the use of attribute data in the data association will reduce the likelihood of this occurring. In fact, the simulations show that the joint kinematic and attribute association algorithm of Section 4.2 [Krieg 2002] forces the track to break at the first manoeuvre and a new track based only on the radar measurements is initiated, thus overcoming the conflict condition. To maintain a continuous track, kinematic only data association is used in this case.

As shown in Figure 19, the probability of class *C2* now falls during the period prior to the manoeuvre, as expected with class measurements supporting a class of *C1*. However, as the target manoeuvres, the probability of class *C2* rises rapidly toward unity. In this case, the evidence provided by the manoeuvre is more significant than the class measurements, which have only an 80% confidence of being correct.

Finally, the effect of the kinematic state estimates on the class probabilities is demonstrated. Three targets are employed in this scenario, one constant velocity, one performing a moderate manoeuvre, and one performing a more demanding manoeuvre. Only the range and bearing measurements of *S1* are available, that is, no class measurements are available. Each target is one of three classes, labelled 1 through 3, where each is able to perform manoeuvres of increasing acceleration.

The estimated position for each target is shown in Figure 20, with 20(a) being the composite track from all three class models, and 20(b) through 20(d) being the individual tracks for each class model. The filter lag during the manoeuvres on the blue track representing the target with the highest acceleration manoeuvre capability is evident for class models 1 and 2, and the same effect is also evident, albeit to a lesser extent, on the red track for class model 1. The composite tracks are dominated by the constant velocity class model prior to the manoeuvres, and by the appropriate class model during and after the manoeuvres. This behaviour is consistent with the class estimation, as illustrated in Figure 21, where 21(a) through 21(c) show the probabilities for classes 1 through 3, respectively. The colours of the lines in these plots correspond to the colours of the tracks in Figure 20. Prior to the manoeuvres, the probability of class 1 increases, as no evidence for the class of each track is available. However, the manoeuvre provides class information, with the probabilities for the correct classes rapidly rising towards unity in each case. This approach favours the model that specifies the manoeuvres with the lowest acceleration, until a target manoeuvre with higher acceleration eliminates those class models specifying manoeuvres with lower acceleration. This is consistent with Bayesian approaches [Ristic & Smets 2005].

7 Conclusions

Bayesian belief networks (BBNs) are an effective method for modelling the uncertain dependencies between continuous and discrete variables. As such, they provide a suitable framework for developing solutions for the target tracking and recognition problem. Algorithms for kinematic and attribute data association and state estimation have been developed using this framework and the advantages of using both kinematic and attribute information has been demonstrated using simulated scenarios.

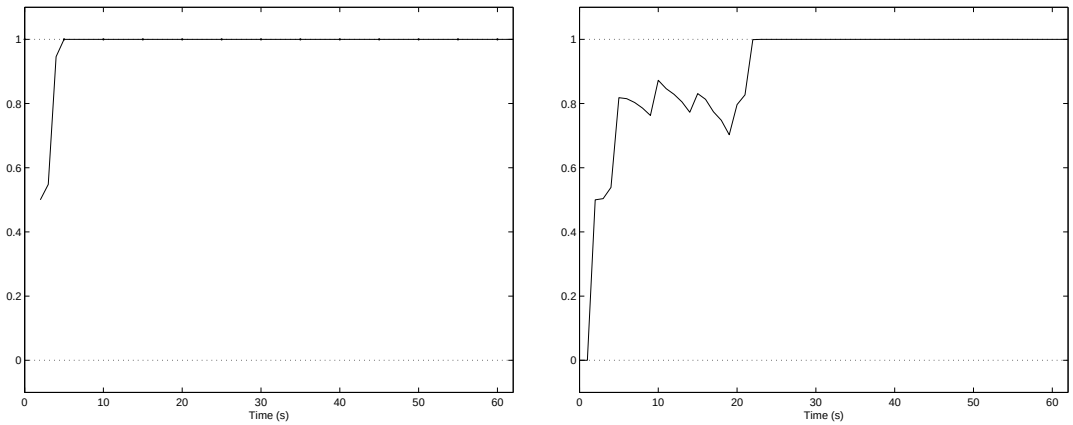

(a) Single run *(b) Mean*

Figure 18: *Probability of class* C2 *from position and class measurements*

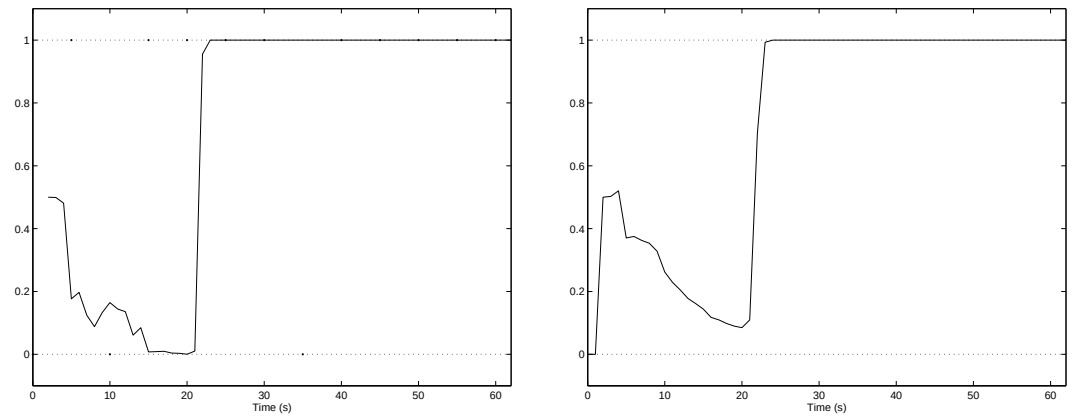

(a) Single run *(b) Mean*

Figure 19: *Probability of class* C2 *from conflicting position and class measurements*

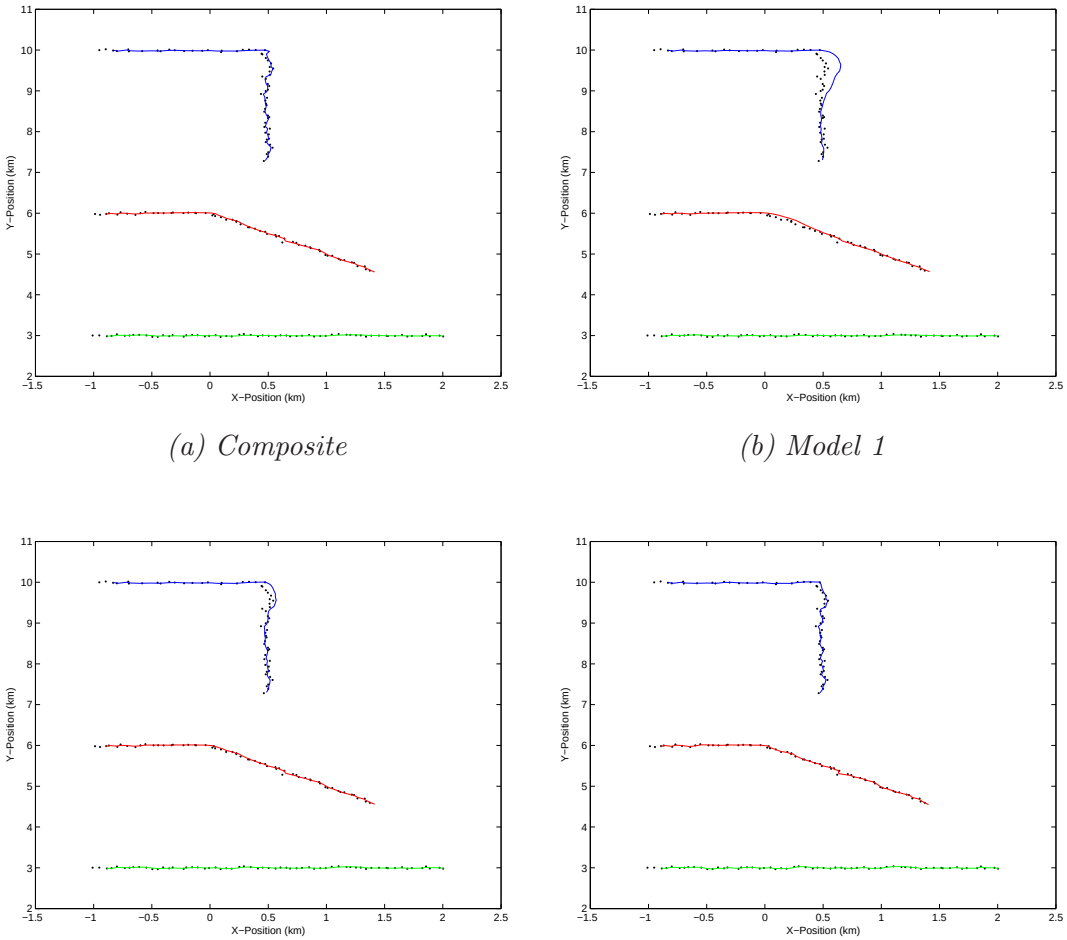

(a) Composite *(b) Model 1*

(c) Model 2 *(d) Model 3*

Figure 20: *Track positions for the three target scenario with only position measurements*

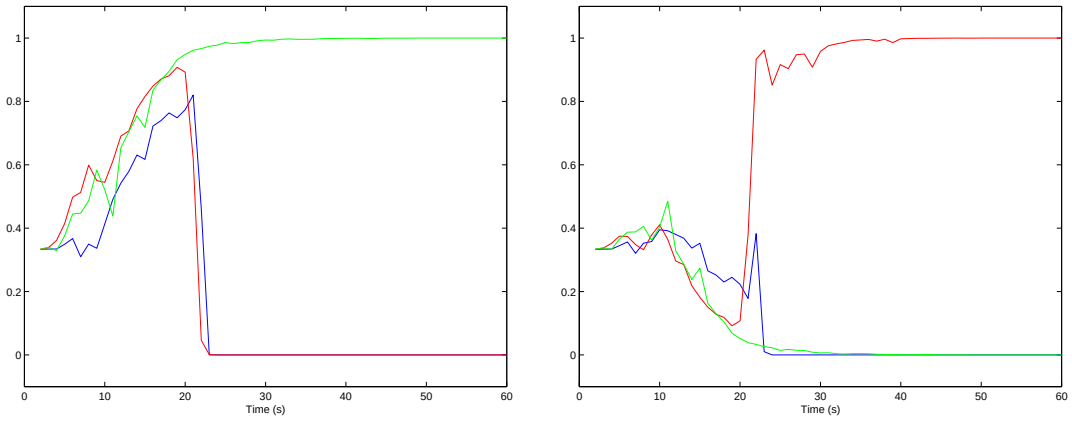

(a) Class 1 *(b) Class 2*

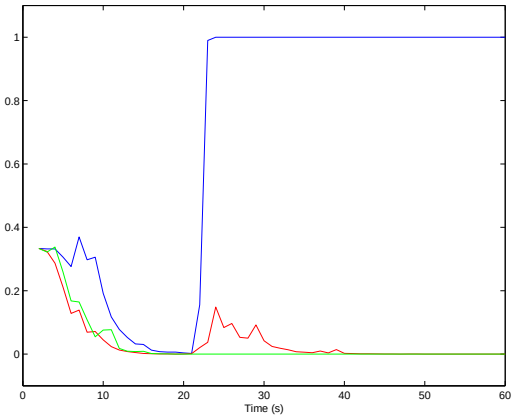

(c) Class 3

Figure 21: *Class probabilities for the three target scenario with only position measurements*

The use of both kinematic and attribute sensor data and target states for data association improves the ability of the algorithms to discriminate between multiple measurements and targets. The resulting improvement in data association performance, particularly in dense target scenarios, has been shown through demonstration to improve kinematic tracking performance. The application of attribute state estimation algorithms that provide accurate estimates of a target's attribute states enhances the data association performance and hence the kinematic tracking performance.

A joint kinematic and attribute tracking algorithm has been developed using a BBN that captures the dependencies between the target's kinematic and attribute states. It has been shown that the target's class or type can be estimated from the kinematic behaviour of the target using this technique. In addition, knowledge of the target's class may improve the kinematic tracking performance through the selection of the most appropriate kinematic model for that class.

Future work may include the development and evaluation of similar algorithms for different sensor mixes, target types and scenarios. In particular, more complex sets of attribute variables, including variables such as platform type and platform specific type, may be developed.

References

Blackman, S. & Popoli, R. (1999) *Design and Analysis of Modern Tracking Systems*, Artech House, Norwood MA.

Bogler, P. L. (1987) Shafer-Dempster reasoning with applications to multisensor target identification systems, *IEEE Transactions on Systems, Man, and Cybernetics* **SMC-17**(6), 968–77.

Challa, S. & Pulford, G. W. (1999) Joint target tracking and classification, *in Proceedings of the 5th International Conference on Radar Systems (Radar '99)*, Brest, France.

Chang, K.-C. & Fung, R. (1997) Target identification with Bayesian networks in a multiple hypothesis tracking system, *Optical Engineering* **36**(3), 684–91.

Gordon, N., Maskell, S. & Kirubarajan, T. (2002) Efficient particle filters for joint tracking and classification, *in Signal and Data Processing of Small Targets 2002*, Vol. 4728 of *Proceedings of the SPIE*, pp. 439–49.

Hautaniemi, S. K., Korpisaari, P. T. & Saarinen, J. P. P. (2000) Target identification with Bayesian networks, *in Sensor Fusion: Architectures, Algorithms, and Applications IV*, Vol. 4051 of *Proceedings of the SPIE*, pp. 55–66.

Jensen, F. V. (1996) *An Introduction to Bayesian Networks*, UCL Press, London UK.

Khosla, D. & Chen, Y. (2003) Joint kinematic and feature tracking using probabilistic argumentation, *in Proceedings of the International Conference on Information Fusion (Fusion 2003)*, Cairns Australia.

Korpisaari, P. & Saarinen, J. (1999) Bayesian networks for target identification and attribute fusion with JPDA, *in Proceedings of the 2nd International Conference on Information Fusion*, Vol. II, International Society of Information Fusion, pp. 763–9.

Krieg, M. L. (2001) *A Tutorial on Bayesian Belief Networks*, Technical Report DSTO–TN–0403, DSTO Australia.

Krieg, M. L. (2002) A Bayesian belief network approach to multi-sensor kinimatic and attribute tracking, *in Proceedings of the Information, Decision and Control Conference (IDC2002)*, Adelaide, Australia, pp. 401–6.

Krieg, M. L. (2003*a*) Joint multi-sensor kinematic and attribute tracking using Bayesian belief networks, *in Proceedings of the International Conference on Information Fusion (Fusion 2003)*, Cairns Australia.

Krieg, M. L. (2003*b*) Multi-sensor kinematic and attribute tracking using a Bayesian belief network, *in NATO IST Panel Symposium on Military Data and Information Fusion*, Prague, Czech Republic.

Pearl, J. (1988) *Probabilistic Reasoning in Intelligent Systems: Networks of Plausible Inference*, Morgan Kaufmann, San Francisco CA.

Ristic, B. & Smets, P. (2005) Target classification approach based on the belief function theory, *IEEE Transactions on Aerospace and Electronic Systems* **41**(2), 574–83.

Simard, M.-A., Couture, J. & Bossé, É. (1996) Data fusion of multiple sensors attribute information for target identity estimation using a Dempster-Shafer evidential combination algorithm, *in Signal and data processing of small targets 1996*, Vol. 2759 of *Proceedings of the SPIE*, pp. 577–88.

Stewart, L. & McCarty, Jr., P. (1992) The use of Bayesian belief networks to fuse continuous and discrete information for target recognition, tracking and situation assessment, *in Signal Processing, Sensor Fusion and Target Recognition*, Vol. 1699 of *Proceedings of the SPIE*, pp. 177–85.

DISTRIBUTION LIST

Kinematic and Attribute Fusion Using a Bayesian Belief Network Framework

Mark L Krieg

	Number of Copies
AUSTRALIA	
DEFENCE ORGANISATION	
Task Sponsor	
Director General Aerospace Development	1 (printed)
S&T Program	
Chief Defence Scientist	1
Deputy Chief Defence Scientist Policy	1
Assistant Secretary Science Corporate Management	1
Director General Science Policy Development	1
Counsellor Defence Science, London	Doc Data Sheet
Counsellor Defence Science, Washington	Doc Data Sheet
Scientific Adviser to MRDC, Thailand	Doc Data Sheet
Scientific Adviser Joint	1
Navy Scientific Adviser	Doc Data Sheet and Dist List
Scientific Adviser, Army	Doc Data Sheet and Dist List
Air Force Scientific Adviser	Doc Data Sheet and Dist List
Scientific Adviser to the DMO	Doc Data Sheet and Dist List
Deputy Chief Defence Scientist Platform and Human Systems	Doc Data Sheet and Dist List
Chief ISRD	Doc Data Sheet and Dist List
Research Leader Information Integration	Doc Data Sheet and Dist List
Task Manager	1
Author	1 (printed)
DSTO Library and Archives	
Library, Edinburgh	1 (printed)
Defence Archives	1 (printed)
Capability Development Group	
Director General Maritime Development	Doc Data Sheet
Director General Capability and Plans	Doc Data Sheet

Assistant Secretary Investment Analysis	Doc Data Sheet
Director Capability Plans and Programming	Doc Data Sheet
Chief Information Officer Group	
Director General Australian Defence Simulation Office	Doc Data Sheet
Assistant Secretary Information Strategy and Futures	Doc Data Sheet
Director General Information Services	Doc Data Sheet
Strategy Group	
Assistant Secretary Strategic Planning	Doc Data Sheet
Assistant Secretary Governance and Counter-Proliferation	Doc Data Sheet
Navy	
Maritime Operational Analysis Centre, Building 89/90, Garden Island, Sydney NSW	
Deputy Director (Operations)	Doc Data Sheet and Dist List
Deputy Director (Analysis)	
Director General Navy Capability, Performance and Plans, Navy Headquarters	Doc Data Sheet
Director General Navy Strategic Policy and Futures, Navy Headquarters	Doc Data Sheet
Air Force	
SO (Science), Headquarters Air Combat Group, RAAF Base, Williamtown NSW	Doc Data Sheet and Exec Summ
Army	
ABCA National Standardisation Officer	
Land Warfare Development Sector, Puckapunyal	Doc Data Sheet (pdf format)
J86 (TCS GROUP), DJFHQ	Doc Data Sheet
SO (Science), Land Headquarters (LHQ), Victoria Barracks, NSW	Doc Data Sheet and Exec Summ
SO (Science), Deployable Joint Force Headquarters (DJFHQ)(L), Enoggera QLD	Doc Data Sheet
Joint Operations Command	
Director General Joint Operations	Doc Data Sheet
Chief of Staff Headquarters Joint Operation Command	Doc Data Sheet
Commandant ADF Warfare Centre	Doc Data Sheet
Director General Strategic Logistics	Doc Data Sheet
COS Australian Defence College	Doc Data Sheet
Intelligence and Security Group	
Assistant Secretary Concepts, Capabilities and Resources	1

DGSTA, Defence Intelligence Organisation	1
Manager, Information Centre, Defence Intelligence Organisation	1
Director Advanced Capabilities	Doc Data Sheet

Defence Materiel Organisation

Deputy CEO, DMO	Doc Data Sheet
Head Aerospace Systems Division	Doc Data Sheet
Head Maritime Systems Division	Doc Data Sheet
Program Manager Air Warfare Destroyer	Doc Data Sheet
Guided Weapon & Explosive Ordnance Branch (GWEO)	Doc Data Sheet
CDR Joint Logistics Command	Doc Data Sheet

OTHER ORGANISATIONS

National Library of Australia	1
NASA (Canberra)	1

UNIVERSITIES AND COLLEGES

Australian Defence Force Academy

Library	1
Head of Aerospace and Mechanical Engineering	1
Hargrave Library, Monash University	Doc Data Sheet

OUTSIDE AUSTRALIA

INTERNATIONAL DEFENCE INFORMATION CENTRES

US Defense Technical Information Center	1
UK DSTL Knowledge Services	1
Canada Defence Research Directorate R&D Knowledge and Information Management (DRDKIM)	1
NZ Defence Information Centre	1

ABSTRACTING AND INFORMATION ORGANISATIONS

Library, Chemical Abstracts Reference Service	1
Engineering Societies Library, US	1
Materials Information, Cambridge Scientific Abstracts, US	1
Documents Librarian, The Center for Research Libraries, US	1

SPARES

DSTO Edinburgh Library	5 (printed)

Total number of copies: printed 9, pdf 21

DEFENCE SCIENCE AND TECHNOLOGY ORGANISATION DOCUMENT CONTROL DATA	1. CAVEAT/PRIVACY MARKING

2. TITLE	3. SECURITY CLASSIFICATION
Kinematic and Attribute Fusion Using a Bayesian Belief Network Framework	Document (U) Title (U) Abstract (U)
4. AUTHOR	5. CORPORATE AUTHOR
Mark L Krieg	Defence Science and Technology Organisation PO Box 1500 Edinburgh, South Australia 5111, Australia

6a. DSTO NUMBER	6b. AR NUMBER	6c. TYPE OF REPORT	7. DOCUMENT DATE
DSTO–RR–0315	013–722	Research Report	August, 2006

8. FILE NUMBER	9. TASK NUMBER	10. SPONSOR	11. No OF PAGES	12. No OF REFS
2006/1052880/1	JTW 05/305	DGAD	38	17

13. URL OF ELECTRONIC VERSION	14. RELEASE AUTHORITY
http://www.dsto.defence.gov.au/corporate/reports/DSTO–RR–0315.pdf	Chief, Intelligence, Surveillance and Reconnaissance Division

15. SECONDARY RELEASE STATEMENT OF THIS DOCUMENT

Approved For Public Release

OVERSEAS ENQUIRIES OUTSIDE STATED LIMITATIONS SHOULD BE REFERRED THROUGH DOCUMENT EXCHANGE, PO BOX 1500, EDINBURGH, SOUTH AUSTRALIA 5111

16. DELIBERATE ANNOUNCEMENT

No Limitations

17. CITATION IN OTHER DOCUMENTS

No Limitations

18. DSTO RESEARCH LIBRARY THESAURUS

Target tracking
Kinematics
Attribute fusion
Target recognition
Bayesian networks

19. ABSTRACT

The focus of tracking applications has traditionally centred on kinematic state estimation. However, attribute information has the potential to not only provide identity and class information, but it may also improve data association and kinematic tracking performance. Bayesian Belief Networks provide a framework for specifying the dependencies between kinematic and attribute states. Algorithms based on this framework are developed for joint kinematic and attribute data association, kinematic tracking, attribute state estimation, and joint kinematic and attribute tracking. The algorithms are demonstrated using simulated tracking scenarios.